

NASA TECHNICAL MEMORANDUM

NASA TM X-64921

(NASA-TM-X-64921) : A TIMELINE ALGORITHM FOR
ASTRONOMY MISSIONS (NASA) : 57 p HC \$4.25
CSCL 03A

N75-22216

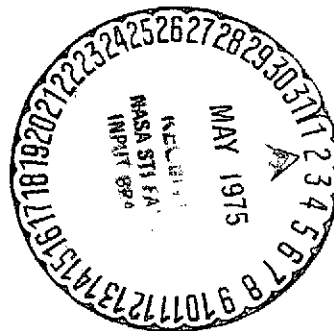
Unclas

63/89 18619

A TIMELINE ALGORITHM FOR ASTRONOMY MISSIONS

By John E. Moore and Orville T. Guffin
Systems Analysis and Integration Laboratory

April 1975



NASA

*George C. Marshall Space Flight Center
Marshall Space Flight Center, Alabama*

1. REPORT NO. NASA TM X-64921		2. GOVERNMENT ACCESSION NO.		3. RECIPIENT'S CATALOG NO.	
4. TITLE AND SUBTITLE A Timeline Algorithm for Astronomy Missions				5. REPORT DATE April 1975	
				6. PERFORMING ORGANIZATION CODE	
7. AUTHOR(S) John Edd Moore and Orville Thomas Guffin				8. PERFORMING ORGANIZATION REPORT #	
9. PERFORMING ORGANIZATION NAME AND ADDRESS George C. Marshall Space Flight Center Marshall Space Flight Center, Alabama 35812				10. WORK UNIT NO.	
				11. CONTRACT OR GRANT NO.	
12. SPONSORING AGENCY NAME AND ADDRESS National Aeronautics and Space Administration Washington, D. C. 20546				13. TYPE OF REPORT & PERIOD COVERED Technical Memorandum	
				14. SPONSORING AGENCY CODE	
15. SUPPLEMENTARY NOTES Prepared by Systems Analysis and Integration Laboratory, Science and Engineering					
16. ABSTRACT This report presents an algorithm for generating viewing timelines for orbital astronomy missions of the pointing (nonsurvey/scan) type. The algorithm establishes a target sequence from a list of candidate targets in a way which maximizes total viewing time. Two special cases are treated. One concerns dim targets which, due to lighting constraints, are scheduled only during the antipolar portion of each orbit. They normally require long observation times extending over several revolutions. A minimum slew heuristic is employed to select the sequence of dim targets. The other case deals with bright, or short duration, targets, which have less restrictive lighting constraints and are scheduled during the portion of each orbit when dim targets cannot be viewed. Since this process moves much more rapidly than the dim path, an enumeration algorithm is used to select the sequence that maximizes total viewing time.					
17. KEY WORDS Scheduling Algorithm Enumeration Technique Astronomy Mission Planning Timeline Algorithm Mathematical Programming Mission Simulation			18. DISTRIBUTION STATEMENT Unclassified - Unlimited <i>for James B. Leichter</i> John Edd Moore		
19. SECURITY CLASSIF. (of this report) Unclassified	20. SECURITY CLASSIF. (of this page) Unclassified	21. NO. OF PAGES 57	22. PRICE NTIS		

TABLE OF CONTENTS

	Page
I. SUMMARY	1
II. INTRODUCTION	1
III. TYPICAL APPLICATION OF ALGORITHM.....	5
A. Input Assumptions and Instrument Characteristics	5
B. Target Modeling	12
C. Operational Mode Scenario and Rationale	12
D. Sample Timelines	19
E. Summary of Results and Statistical Analysis.....	27
IV. CONCLUSIONS	29
APPENDIX — AN ALGORITHM FOR A SINGLE MACHINE SCHEDULING PROBLEM WITH SEQUENCE DEPENDENT SETUP TIMES AND SCHEDULING WINDOWS	36
REFERENCES.....	51

PRECEDING PAGE BLANK NOT FILMED

LIST OF ILLUSTRATIONS

Figure	Title	Page
1.	Integration time curve, high resolution (f/24) camera	7
2.	Integration time curves — faint object spectrographs	8
3.	Integration time curves — high resolution spectrographs . . .	9
4.	Integration time curves — IR instrument, photometer, and astrometer	10
5.	General regions of interest in the celestial sphere and faint and bright target areas in timeline	13
6.	Aitoff-Hammer projection of isochronic viewing contours in ecliptic coordinates for 25th magnitude targets on day 1 . .	18
7.	Option 1 timeline, TL-4	21
8.	Option 2 timeline, TL-5	29
9.	Distribution of targets scheduled in TL-4 according to magnitude	30
10.	Distribution of targets scheduled in TL-5 according to magnitude	31
11.	Distribution of observation times for TL-4	32
12.	Distribution of observation times for TL-5	33
13.	Distribution of slew times for TL-4	34
14.	Distribution of slew times for TL-5	35

LIST OF TABLES

Table	Title	Page
1.	Instrument Characteristics Assumed	6
2.	Instrument Complement Matrix	11
3.	Pseudo-Targets Scheduled, Options 1 and 2	14
4.	Summary of Results for 2 Days (31 Orbits) of Observations	28

A TIMELINE ALGORITHM FOR ASTRONOMY MISSIONS

I. SUMMARY

An algorithm is presented for generating viewing timelines for orbital astronomy missions of the pointing (nonsurvey/scan) type. The algorithm establishes a target sequence from a list of candidate targets in a way which maximizes total viewing time. Due to lighting constraints, dim targets are scheduled only during the antisolar portion of each orbit. They require long observation times extending over several orbits. The viewing of one dim target is completed before the next dim target is scheduled. Brighter targets, which have less restrictive lighting conditions, are scheduled during the portion of each orbit when the dim target cannot be viewed. Usually, the viewing requirements of two or more bright targets can be completed during this part of the orbit. An enumeration algorithm described in the appendix is employed to select these targets. A minimum slew heuristic is employed to select the sequence of dim targets to be viewed. A complete description of the algorithm is provided by Section II.

Application of the algorithm to the Large Space Telescope (LST) program is discussed in Section III. The LST timelines illustrate the full capability of the algorithm and how it can be used to simulate and/or schedule complex space astronomy missions.

II. INTRODUCTION

The timeline algorithm presented in this report was originally developed for the LST program but is now applied also to other spacecraft and astronomy missions of the pointing (nonsurvey/scan) type. This algorithm determines a target sequence, or viewing path, from a list of candidate sources in such a way that total viewing time over a specified portion of the mission is maximized while maintaining a uniform distribution of target magnitude.

The selection of an optimal path is typically restricted by orbital lighting conditions, by the time intervals each star can be seen, by the observation time required for a given star and sensor, and by observational philosophy itself. For example, viewing requirements for faint targets are normally longer than one interval, so a number of revolutions are required to complete observation. In addition, stray light constraints make it preferable, if not necessary, to view dim sources on the antisolar side of an orbit. This may be either strictly the orbital shadow interval or, in the case of telescopes equipped with sunshades and baffling systems, a longer interval centered around orbital midnight. Philosophy enters at this point in formulating approaches to the space observatory scheduling problem which will yield high mission utility, low program cost, and maximum scientific return. Subsystem capabilities, instrument sensitivities, and target dwell times are the primary factors that influence the selection of a specific approach.

The LST, for instance, is designed to observe very dim sources, which, in turn, requires very long observation times extending over many revolutions. The large dynamic range which makes this possible, however, results in very short times for relatively bright objects. The problem of how to mix such a wide diversity of times in the most efficient manner is the key to the logic developed in the algorithm. As originally conceived, the LST had the ability for relatively fast slewing, making it possible to supplement the viewing program with brighter targets during periods of prime region occultation. This allowed a separation of the brighter targets from the very faint into two distinct portions of each revolution; i. e., the portion centered around orbital midnight is reserved for faint sources and all other sources are scheduled within the remaining portion. Restricting observations in this manner is equivalent to dividing the very long viewing times from the short.

Since the viewing of faint sources is one of the primary LST objectives, any scheduling technique should provide as much faint source viewing as possible. This can be accomplished by beginning observation of a dim target as soon as it is viewable each dark-side pass and continuing observation of the current dim target until it is lost from view. In addition, by applying the time restriction from the previous paragraph and by slewing to subsequent dim targets requiring the minimum maneuver time, primary viewing will attain the highest possible efficiency. Since slewing between primary targets would then be infrequent, this portion of each revolution can be made very efficient.

This scheme implies, of course, that either there is little interest in observing brighter sources or that the spacecraft/instrument platform has a sufficiently high slew rate capability to provide secondary viewing on the bright

side of each revolution. A number of Spacelab payloads and the 3 m class LST design do have this capability. The current LST redesigns with their small and inexpensive pointing and control systems, on the other hand, render secondary viewing all but impossible. In this case a somewhat different approach must be taken.

Although the scheduling algorithm can be applied more generally, the specific approach modeled in this report follows the secondary viewing scheme described above. Target acquisition/loss intervals based on stray light constraints and occultations are calculated by another routine and fed into the scheduling model by tape. Candidate targets are divided into two classes for each instrument complement: one for faint sources viewed on the antisolar side and one for supplementary bright-side viewing. The telescope returns to the current primary target every dark-side pass until the required observation time is satisfied and then slews to the next dim target requiring the smallest maneuver time. Observation times are calculated by summing integration times from input curves over the instrument complement scheduled. Secondary viewing, on the bright side, is determined by the algorithm, which maximizes total viewing time while minimizing losses due to slewing and unused time. The slew from the primary to the secondary region is not permitted until the primary target is lost from view, and the telescope must slew back and be ready to view the primary target again (or next dim target) as soon as it is available. The current primary target then sets the begin and end point of the bright-side target path.

The algorithm, therefore, performs two distinct tasks: (1) selects a sequence of faint sources over a given mission segment and (2) determines optimum bright-side viewing paths that fit between the dark-side viewing paths. The latter is achieved by implicitly enumerating all possible and promising paths, making use of fathoming tests for eliminating nonpromising paths to find the one with the best objective value. Notice that the primary target path is independent of the bright-side path and is, therefore, the same regardless of the presence or absence of secondary viewing. In addition, bright side paths have no effect on each other (except the diminishing list of candidate targets as they are scheduled), so substitution or deletion of scheduled targets does not require a completely new timeline.

Although this scheme produces high observation efficiency, it does have several drawbacks. For example, the slews within a target region can be made quite small, but the two slews per revolution connecting the primary and secondary regions are of necessity relatively large to avoid earth occultation. This means that the pointing/control system must provide much more slewing (magnitude and frequency) than would be necessary for dark-side-only viewing.

In the case of free flying satellites, such as LST, this is a significant design factor but, for pallet-mounted telescopes on the Shuttle, this is of little consequence. Another disadvantage is some additional complication in data management, since the approach implies a separation of "dim" and "bright" target data. The impact of this problem, however, is softened if bright-side targets are restricted to single-pass observation, so only the faint source memory needs to keep track of subsequent revolutions.

In cases where this "multitarget" viewing is not attainable (e.g., the 2 m class LST redesign offers a slew rate so slow that supplementary viewing is virtually eliminated), the dark-side viewing interval should be "stretched" as much as possible with protection devices such as sunshades and baffles and efficient use should be made of the available time. The remainder of each revolution would then be used for data transmission, subsystem monitoring, solar array reorientation, antennae positioning, instrument preparation, etc., and any other spacecraft functions that are inhibited during observation. Since "short" and "long" viewing times are no longer divided into separate intervals, efficiency can be maintained by determining an acceptable range of "mixture ratios" (short observations/long observations) which will keep slew losses to a minimum.

Other schedule philosophies are possible but will not be discussed here since they are beyond the scope of this report.

The sequence of faint sources is determined by a simple heuristic. The first target in the sequence is either specified by the user, is the earliest available source, or is determined from the position of the previous target. The next target is selected by listing all the candidate sources that are visible at the time viewing of the first source will end and, from this set, choosing the target requiring the minimum slew time. In general, then, the $(k + 1)$ target in the sequence is the target requiring the minimum slew time from the k th source which also belongs to the set of targets in view at the time viewing of the k th source is completed.

Since the faint target path is a relatively slow moving affair, the total efficiency of each revolution will depend primarily on the secondary viewing path selection. An optimization procedure has been developed to assure that the selected target sequences achieve the highest possible efficiency. The techniques of integer linear programming are used to search the feasible viewing paths to find the one which maximizes path value. An input value is assigned to each candidate source and is used in a function which determines path value. This function increases with weighted observation time and decreases with slew

time and waiting time (unused time at end of bright side). Any weighted values can be assigned to each target, but the experience gained from a statistical analysis of this parameter with random target samples and a number of mission studies indicates that equating the weight to required viewing time results in both the maximum total viewing time and a uniform, unbiased distribution of source magnitudes (equivalent to observation times). The statistical analysis also showed that the function described above consistently out-performed and was less biased than functions which either maximized total viewing time or minimized slewing time only.

A detailed description of the optimization technique is provided in the appendix.

III. TYPICAL APPLICATION OF ALGORITHM

One of the first applications of this algorithm was in timeline simulations for an LST Design Reference Mission (DRM) document which was to have been published in September 1974. Although the LST program experienced a major redefinition shortly before this time and the document was never published, the timelines generated for it illustrate the full capability of the algorithm and the manner in which it can be used to simulate and/or schedule complex space astronomy missions. The input conditions, instrument and target modeling, schedule rationale, sample timelines, and some of the statistical results are discussed in this section.

A. Input Assumptions and Instrument Characteristics

The first step in the simulation process was to set down the operational assumptions and construct the instrument package math model used by the computer. A total of nine instruments were defined, eight of which were science instruments, while one, the target acquisition camera (Slit Jaw Camera), was an auxiliary element. Characteristics of these fictitious instruments are presented in Table 1. The arbitrary devision of the spectrographs into pairs was motivated by a desire to simulate sensors with different spectral ranges. Estimated integration time curves for each instrument are shown in Figures 1 through 4. These curves, which are input to the program by curve fit equations, define how long given sensors must observe targets of given magnitude to obtain one high quality data frame. Times ranged from a maximum of 10 hr to < 1 min. A constant 10 min operation was assigned to the Slit Jaw Camera (SJC), which was required with any complement including a spectrograph.

TABLE 1. INSTRUMENT CHARACTERISTICS ASSUMED

Instrument Name	Abbreviation	Magnitude Range	Power (watts)	Maximum Data Requirement (bits/frame)
High Resolution Camera (f/24)	HRC	≤ 25 25-30	90 105	2×10^8
Faint Object Spectrograph	FOS-1 FOS-2	10-19 12-24	105 135	2×10^8 2×10^8
High Resolution Spectrograph	HRS-1 HRS-2	7-14 7-16	105 135	2×10^8 2×10^8
Photometer	PHOT.	≤ 30	28	6×10^7
Astrometer	ASTR.	≤ 20	15	5×10^7
Infrared	IR	≤ 22	2.2	1×10^4
Slit Jaw Camera (Target Acquisition Camera)	SJC (TAC)	≤ 30	40	2×10^5

It was assumed that the high resolution camera (HRC) could operate simultaneously with any other science instrument but that all other sensors in a specific complement would operate in series. In other words, associated with each target is at least one array of sensors, each of which will record a data frame. If the HRC is involved, it will operate at the same time with one of the other instruments. Thereafter, the remaining sensors will operate one at a time until all desired data are collected on the target. In scheduling observations, the program will sum the integration times for each instrument in the complement, adding any specified time gaps between instruments (for switching, calibration, filter change, etc.). The total time resulting from this calculation is the time that the scheduler routine must allow for this target. With 8 science instruments there are 255 possible complements, the number of instruments in a complement ranging from 1 to 8. Of this total, however, many seem unlikely and would be rarely, if ever, used. For this reason a total of 33 complements with up to 5 instruments each were selected; these complements

ORIGINAL PAGE IS
OF POOR QUALITY

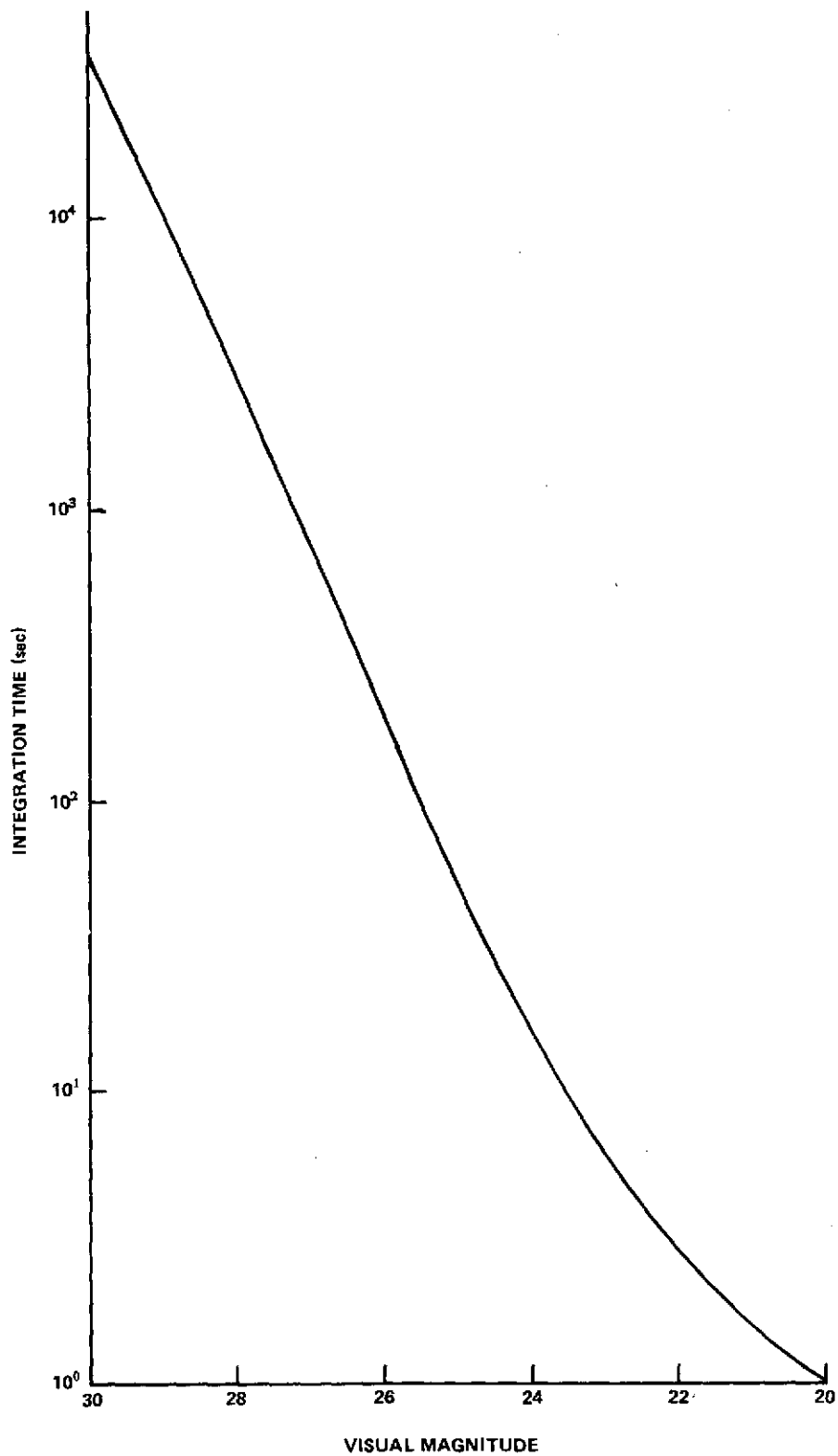


Figure 1. Integration time curve, high resolution (f/24) camera.

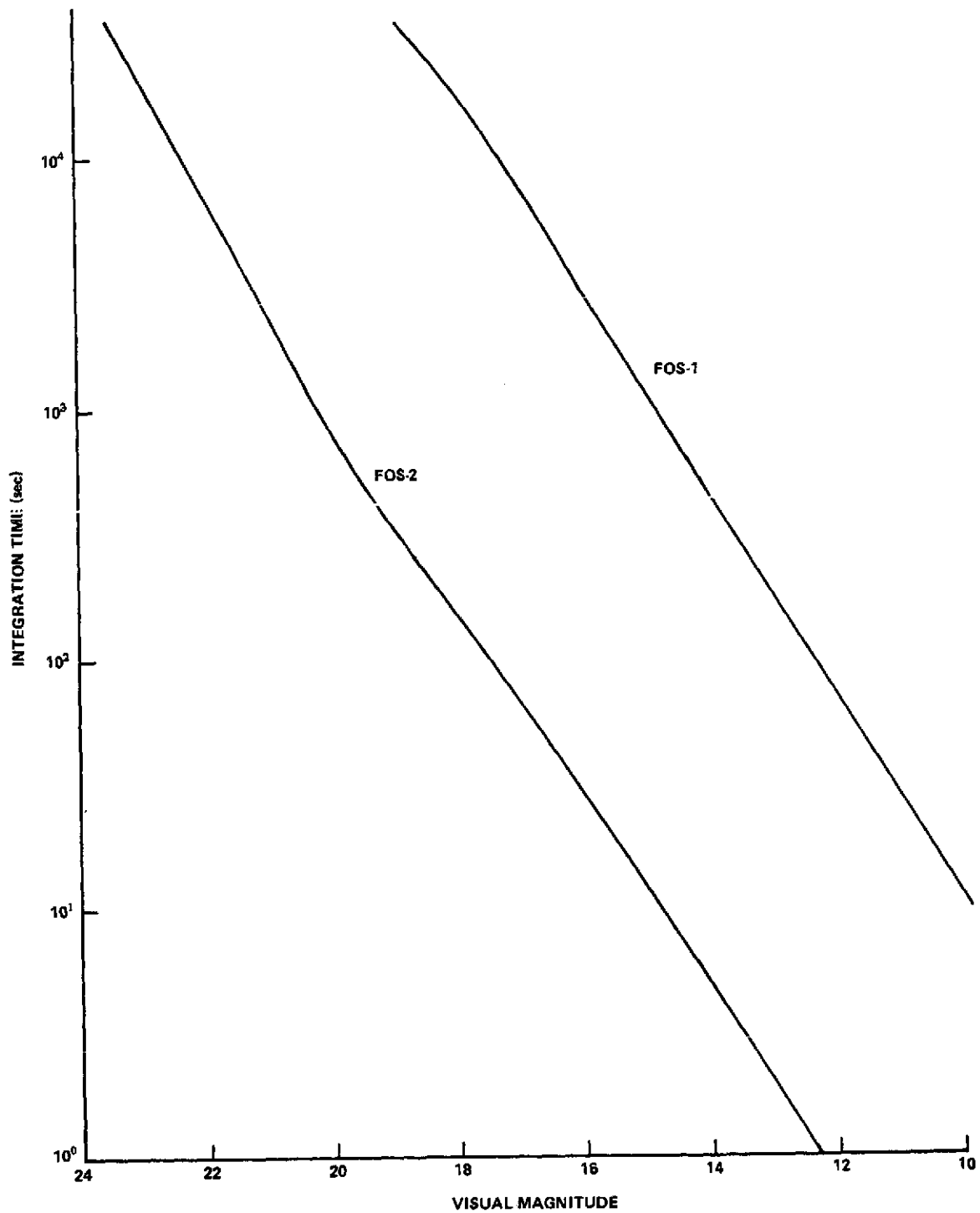


Figure 2. Integration time curves — faint object spectrographs.

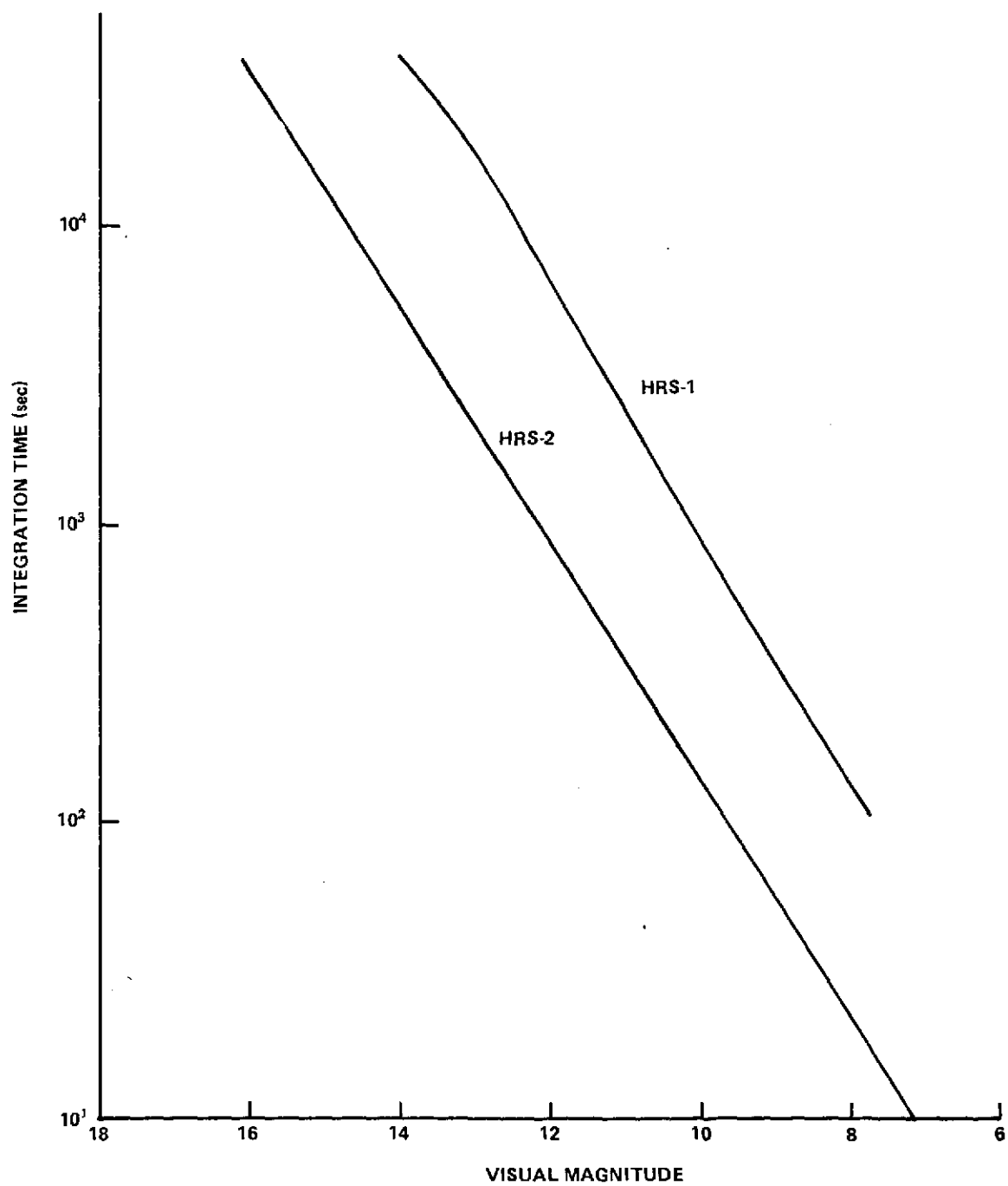


Figure 3. Integration time curves — high resolution spectrographs.

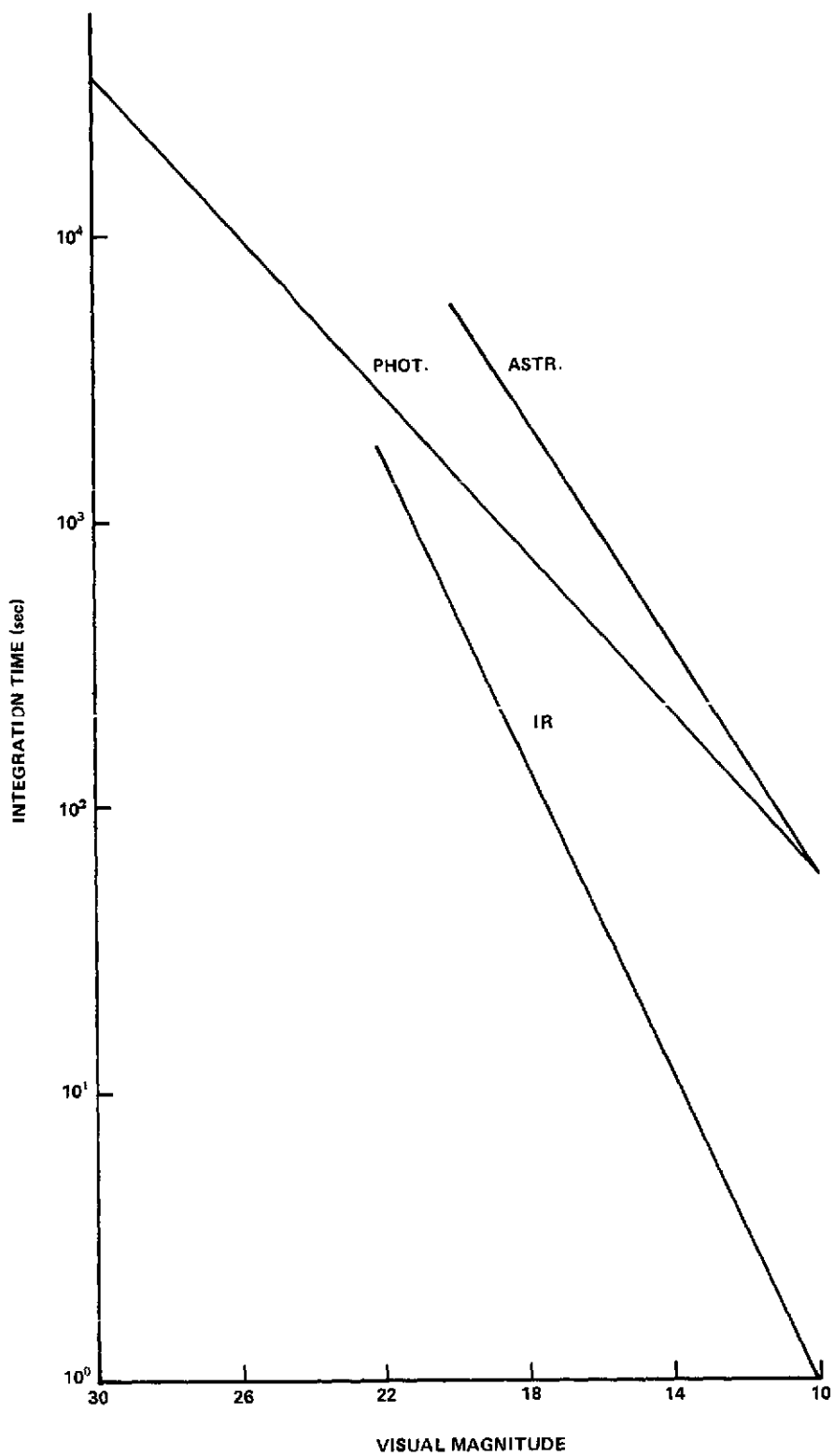


Figure 4. Integration time curves — IR instrument, photometer, and astrometer.

are defined in Table 2. This list is by no means exhaustive but covers a wide range of possibilities. Each grouping appeared likely for relatively frequent use.

TABLE 2. INSTRUMENT COMPLEMENT MATRIX

Complement Code	HRC	FOS-1	FOS-2	HRS-1	HRS-2	Phot.	Astr.	IR	SJC (TAC)
A		X							X
B			X						X
C				X					X
D					X				X
E								X	
F						X			
G	X								
H							X		
I	X	X							X
J	X		X						X
K	X	X						X	X
L	X		X				X		X
M	X			X					X
N	X				X				X
O	X			X			X		X
P	X				X		X		X
Q	X					X			
R	X					X	X		
S	X							X	
T	X						X	X	
U	X						X		
V	X	X	X						X
W	X			X	X				X
X	X					X		X	
Y	X					X	X	X	
Z	X	X				X			X
A'	X		X			X			X
B'	X			X		X			X
C'	X				X	X			X
D'	X			X	X		X		X
E'	X	X	X			X		X	X
F'	X	X						X	X
G'	X			X				X	X

B. Target Modeling

The 350 candidate targets fed to the computer were all pseudo-targets generated by an auxiliary random number program; i.e., any resemblance between one of these targets and a real heavenly body is purely coincidental. Use of pseudo-targets has a number of advantages: (1) any model of the celestial sphere or portion thereof can be simulated without bias, (2) it is much faster than digging from star catalogs, (3) large gaps in existing data can be filled (e.g., very faint objects), and (4) it eliminates the emotional involvement sometimes encountered with real heavenly bodies.

Fifty of the targets were designated as "faint" and generated in the anti-solar region depicted in Figure 5. The remaining targets were "bright" and taken from the rectangular areas close to the sun constraint circle also shown in the same figure. These three sky areas represent the best "viewing windows" for faint and bright targets, respectively, during the 2 day period of the enclosed timelines.

All objects were invented at random locations within each area and given random integer visual magnitudes. "Brights" were assumed to vary between $m_v = 10$ and $m_v = 22$, while "faints" varied from $m_v = 23$ to $m_v = 29$. No magnitude brighter than 10 was used because (1) integration times at this magnitude for most of the sensors are already ≤ 1 min and (2) the LST will probably have little interest in objects brighter than this. One-third of the pseudo-targets were randomly classified as UV only, one-third as IR only, and one-third observable throughout the LST spectral range.

The final step in the input construction was to assign an instrument complement to each target. This was done arbitrarily, but within spectral constraints so that each complement was represented by at least one target. Each of the targets scheduled in the timelines is defined in Table 3.

C. Operational Mode Scenario and Rationale

The isochronal viewing contours shown in Figure 6 define the total time per orbital revolution that an object can be viewed within stray light constraints. These constraints are determined by the amount of extraneous light that can be tolerated at the focal plane and maintain an image of given quality for a specific sensor. The amount of stray light at the focal plane, in turn, is a function of star magnitude, baffle design, sun shade design, zodiacal light level, and vehicle orientation relative to the sun, moon, and bright earth.

TABLE 3. PSEUDO-TARGETS SCHEDULED, OPTIONS 1 AND 2
(Listed in Scheduled Order)

Target No.	R. A. (deg)	Declination (deg)	Visual Magnitude	Spectral Type	Instrument Complement
50	62.092	77.526	28	IR	Q
130	221.533	29.021	11	UV	A
263	317.608	4.151	13	Comb.	Y
113	224.235	27.948	13	IR	Y
209	318.520	-2.511	15	UV	Q
237	317.357	0.257	11	IR	E
66	213.839	22.756	15	UV	Q
72	220.797	23.147	11	UV	U
305	331.809	2.678	15	Comb.	X
59	220.539	22.116	15	UV	Q
71	221.218	23.823	11	Comb.	X
216	324.570	-4.016	15	UV	Q
155	208.280	31.282	15	IR	X
214	322.772	-4.134	15	UV	F
215	323.577	-3.833	22	UV	G
64	215.634	22.065	15	UV	F
226	325.089	-3.296	14	UV	Q
272	328.203	1.331	15	IR	E
73	219.668	23.927	15	IR	T
319	323.905	6.162	12	Comb.	Y
3	77.760	56.802	24	IR	Q
169	218.361	32.136	12	Comb.	Y
321	326.428	5.781	14	UV	Q
76	213.551	23.602	14	UV	Q
247	322.841	-0.966	12	UV	Q

TABLE 3. (Continued)

Target No.	R. A. (deg)	Declination (deg)	Visual Magnitude	Spectral Type	Instrument Complement
298	324.013	5.697	18	UV	G
12	78.189	58.289	24	IR	Q
56	195.464	21.039	12	Comb.	Y
304	330.007	3.001	11	Comb.	Y
111	197.603	26.638	14	UV	X
244	316.972	1.425	12	UV	U
224	321.331	-1.812	17	Comb.	S
13	76.145	58.402	26	IR	Q
171	215.413	32.629	14	Comb.	Q
225	322.583	-3.071	17	Comb.	S
212	321.644	-3.329	16	IR	E
154	210.406	31.089	11	Comb.	Y
230	335.863	-6.204	13	UV	F
97	216.714	25.076	12	UV	Q
62	217.071	22.448	16	IR	E
337	317.357	0.257	11	IR	T
99	213.990	25.812	16	Comb.	Q
222	318.673	-1.464	11	UV	U
221	318.562	-0.694	11	Comb.	X
21	73.313	60.757	23	IR	J
187	196.220	33.792	12	Comb.	T
261	339.848	-3.967	14	Comb.	X
80	201.407	23.654	13	Comb.	F
283	335.919	-0.504	12	Comb.	X
284	337.636	-0.813	15	IR	E

TABLE 3. (Continued)

Target No.	R. A. (deg)	Declination (deg)	Visual Magnitude	Spectral Type	Instrument Complement
94	223.713	25.188	12	IR	U
206	340.807	-9.821	12	Comb.	Y
74	217.955	23.766	17	Comb.	S
89	218.696	24.260	15	IR	E
286	341.935	-1.888	12	UV	Q
75	216.208	23.006	17	Comb.	S
95	221.736	25.281	15	IR	E
307	332.962	2.273	11	UV	U
275	334.012	-0.485	20	UV	G
163	190.385	31.088	16	Comb.	Q
342	331.479	5.757	11	UV	U
343	333.088	5.384	14	IR	E
133	202.754	29.225	12	Comb.	X
234	344.080	-7.588	11	UV	U
233	342.403	-7.143	13	IR	E
20	74.164	60.375	26	IR	Q
136	195.690	29.048	12	UV	Q
313	346.770	-0.519	10	UV	Q
192	209.674	34.148	11	UV	U
165	222.116	32.951	10	IR	R
231	336.237	-6.731	11	Comb.	X
232	339.407	-7.103	19	UV	G
157	206.855	31.199	11	UV	U
227	329.583	-4.744	17	Comb.	S
217	327.997	-5.545	14	IR	E

TABLE 3. (Concluded)

Target No.	R.A. (deg)	Declination (deg)	Visual Magnitude	Spectral Type	Instrument Complement
84	192.370	23.735	11	UV	U
220	345.217	-8.990	17	Comb.	S
19	77.054	60.845	26	IR	Q
81	200.888	23.219	11	UV	X
79	203.010	23.881	14	IR	E
315	321.233	8.073	10	UV	R
254	316.589	2.908	19	UV	G
70	190.958	22.492	17	Comb.	S
53	205.793	21.297	14	IR	E
208	315.871	-0.800	22	UV	G
77	208.411	23.535	17	Comb.	S
67	209.815	22.324	14	IR	E
218	329.735	-5.739	20	UV	G
28	73.117	62.950	25	IR	Q
101	197.000	25.777	18	UV	G
318	323.015	6.961	18	UV	G

The exact size, shape, and position of the isochronal contours varies, but they all show that the maximum available viewing time per revolution for any object exists in a region centered around the antisolar point and that the maximum time an object can be continuously observed per revolution is approximately 45 to 52 min (depending on magnitude). The antisolar point, of course, moves across the sky at the same rate as the sun and is opposite in declination and right ascension. The size of the maximum viewing region decreases as object magnitude becomes fainter, and contours outside this region tend to merge with it.

Also moving with the sun is the zodiacal light, the primary source of unwanted diffuse background light [1]. At any given time two symmetric regions exist centered ~ 65 deg north and south of the antisolar point, where the

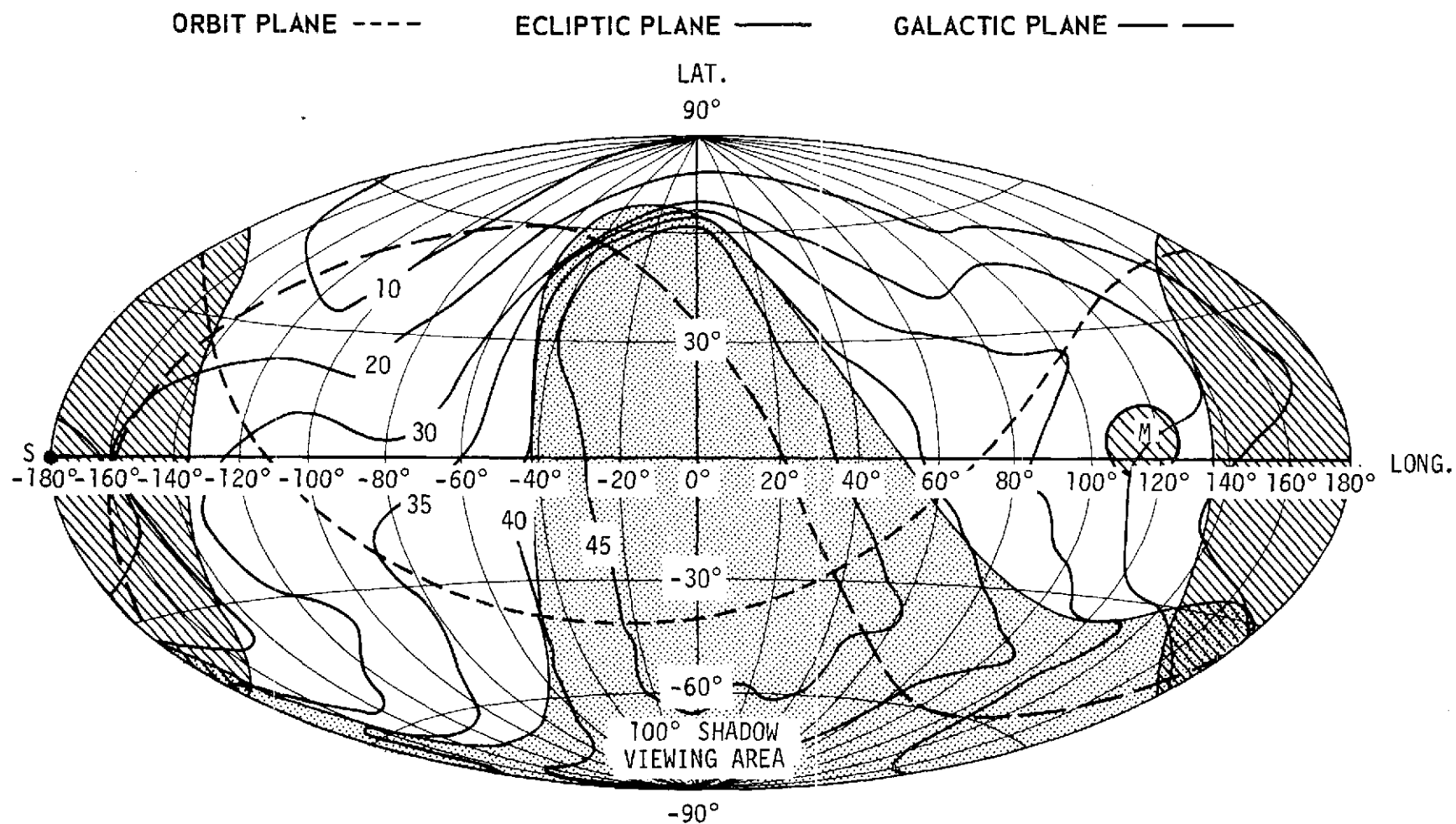


Figure 6. Aitoff-Hammer projection of isochronic viewing contours in ecliptic coordinates for 25th magnitude targets on day 1.

zodiacal light levels are at a minimum. When possible, viewing of faint objects outside the two $S_{10(vis)} \leq 100$ contours should be avoided, since this is the approximate level at which integration times begin to increase as a result of background light. These regions are roughly circular, subtending half cone angles of about 40 deg and are symmetric with respect to the ecliptic plane.

If these contours are superimposed on the isochronal line, the maximum viewing region is cut into two smaller regions north and south of the antisolar point. Prime time viewing of faint objects, then, is most efficiently accomplished on the antisolar side of the orbit and within one of these resultant regions. This is especially important since an increase in the already long integration times required for faint sources will accumulate a large amount of wasted time and a possible degradation in the data. For example, a 29th magnitude star viewed at $S_{10(vis)} = 150$ may require an estimated 15 to 20 percent longer observation time.

The natural progression of the sun will favor different sections of the sky at different times of the year. Targets outside of the area swept out during the yearly cycle, if any, would be viewed when they come closest to one of the prime viewing areas.

D. Sample Timelines

Sample pages from two LST timelines are presented in Figures 7 and 8 to illustrate program capability and the type of information that can be derived from a timeline analysis. Both timelines represent the same mission segment and the same input conditions. The only difference between them lies in the number of secondary viewing regions employed.

Option 1, dubbed TL-4 (timeline #4), scheduled targets in the prime (A) and secondary (B) areas depicted in Figure 5. Option 2, or TL-5, made use of a third area (C) on the opposite side of the sun from area B. Both secondary regions are "twin brothers" and are symmetric with respect to the orbit plane. To eliminate any bias in scheduling between these two areas, the pseudo-targets generated for B were mapped into C and assigned the same instrument complements.

The reason for option 2 was that the stray light constraint characteristics that were modeled did not permit target intervals throughout the entire bright side of each revolution. Region B will provide observation opportunities through

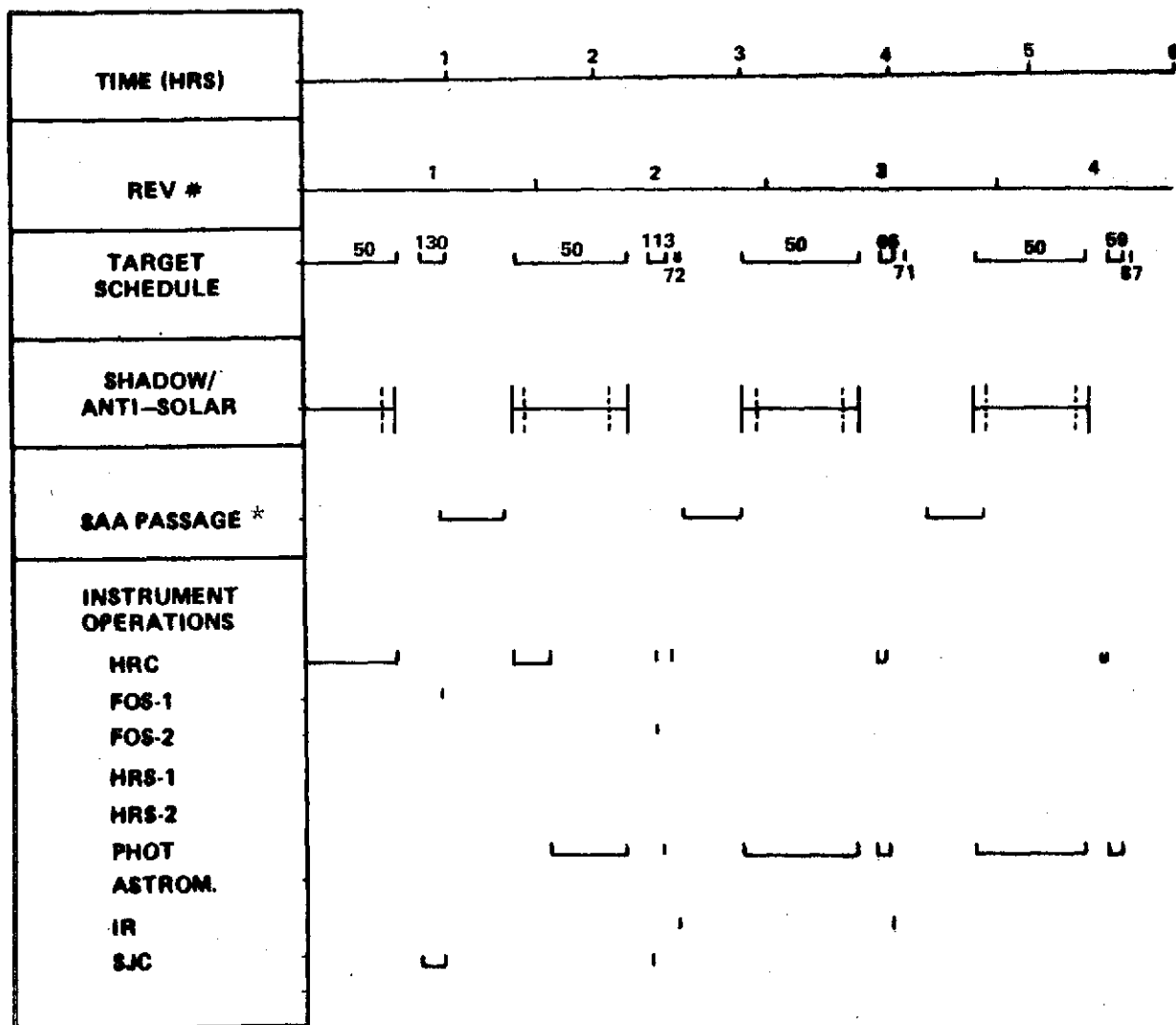
only the first three-fifths of the bright side; similarly, region C covers the last three-fifths, so that the use of B and C together gives continuous coverage for secondary viewing. Since these areas required a major connecting slew, the objective was to compare the differences in efficiency and slew time between the two timelines.

Each timeline is presented in a three page format. The first page contains the target schedule, orbital reference data, radiation passage, and instrument operations; the second page depicts spacecraft attitude, slewing information, and a revolution-by-revolution observation efficiency histogram; the final page shows the power and data rate profiles resulting from the instrument operations.

Orbital revolution number shown on the first page is referenced from one ascending node to the next. The numbers on the target schedule line specify the target under observation. For the characteristics of these pseudo-targets refer to Table 3. The instrument complement codes in the tables are defined in the matrix of Table 2. The fourth line depicts the prime viewing interval of each revolution; the solid lines enclose the antisolar side of the orbit, and the dotted lines bound the actual shadow interval. Line five indicates when the LST passes through the 10 protons/cm²/sec, ≥ 50 MeV level of the South Atlantic Anomaly. The last group of lines on the page show which instrument(s) is taking data.

LST interial attitude is depicted on the second page in terms of right ascension and declination of the target being observed. The next two lines give the size and duration of each slew maneuver and a running average of slew angle. All slews were eigenaxis since this type of maneuver requires minimum time and momentum. A 2 min settle time was deducted after every slew to allow for fine alignment and damping of transient motion. The final line on this page is a revolution-by-revolution histogram of observation efficiency; i.e., the percentage of the orbital period spent observing. Each revolution here is referenced from the beginning of one antisolar interval to the next.

The last page of the timeline format depicts the power and data rate profiles resulting from the observatory schedules. A standby power of 1500 watts was assumed for the total LST system, so that the variation in the profile is due to the observation program. Since all instruments require long warmup times and since their standby power is low, all instruments were assumed to be on during the entire mission segment. The data profiles were based on the total bits required for a frame of data on each instrument given in the last column of Table 1. These numbers are divided by the observation times to determine an average rate that will produce the desired number of bits at the end of the observation. Other buildup schemes could be employed to simulate more realistically the data management path from detector to memory, but the present profiles are sufficient to produce accurate data storage profiles.



*SOUTH ATLANTIC ANOMALY, 10 PROTONS/cm²/sec, ≥ 50 MeV

NOTE: EACH 6 HOUR MISSION SEGMENT IS PRESENTED IN A THREE PAGE FORMAT.

Figure 7. Option 1 timeline, TL-4.

ORIGINAL PAGE IS
OF POOR QUALITY

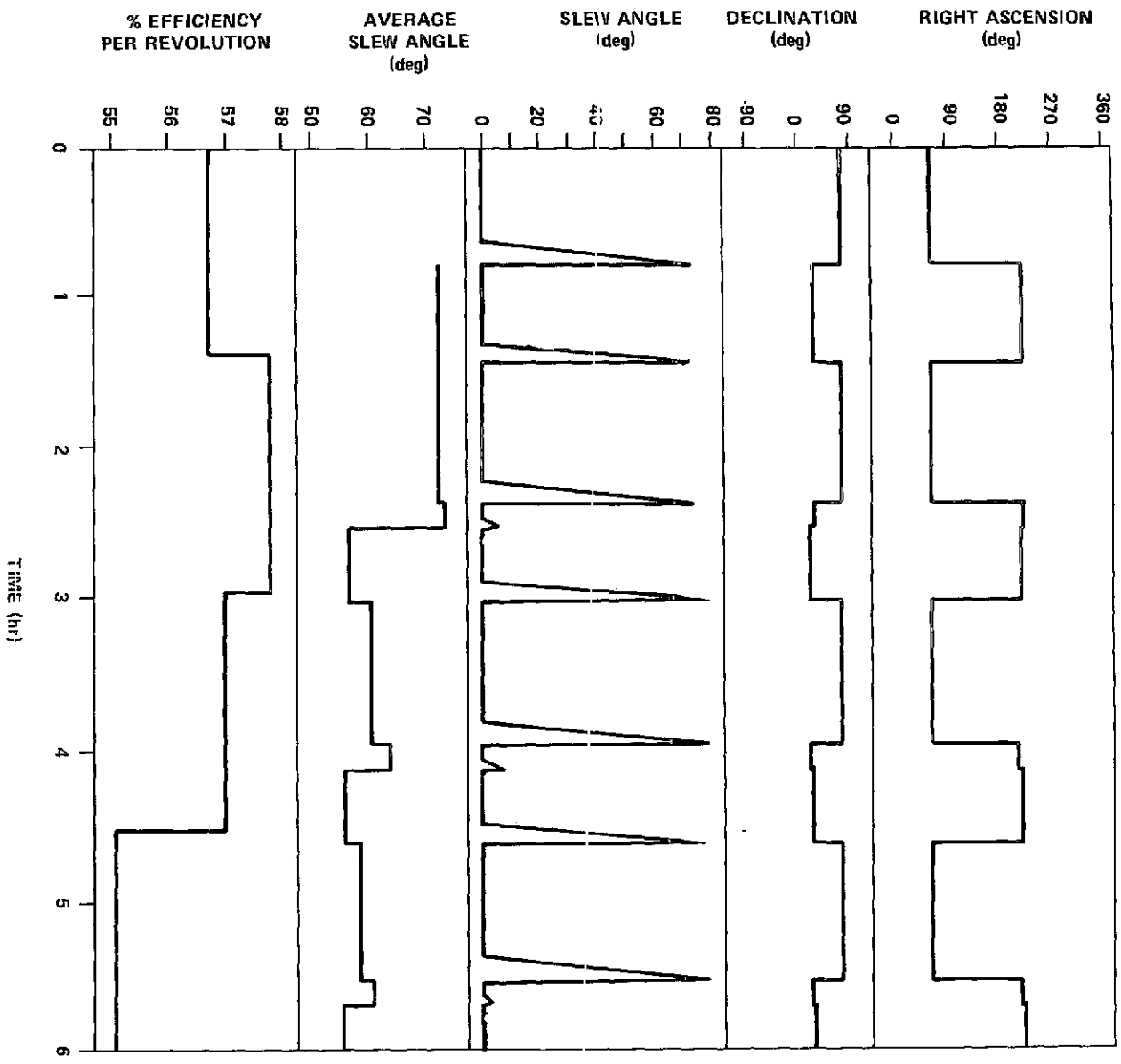


Figure 7. (Continued).

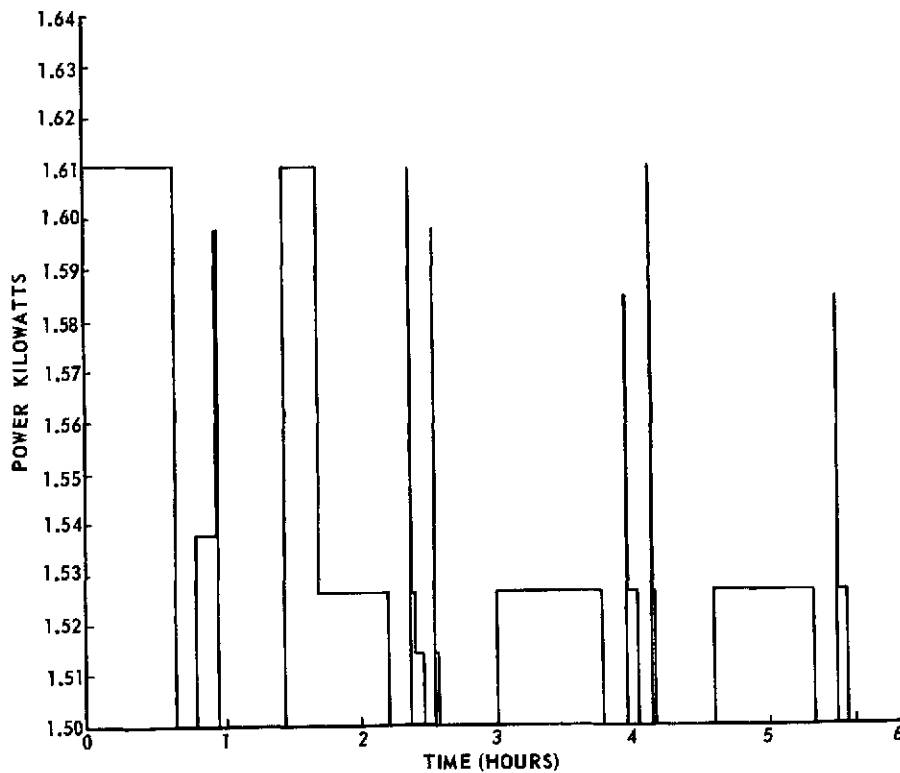
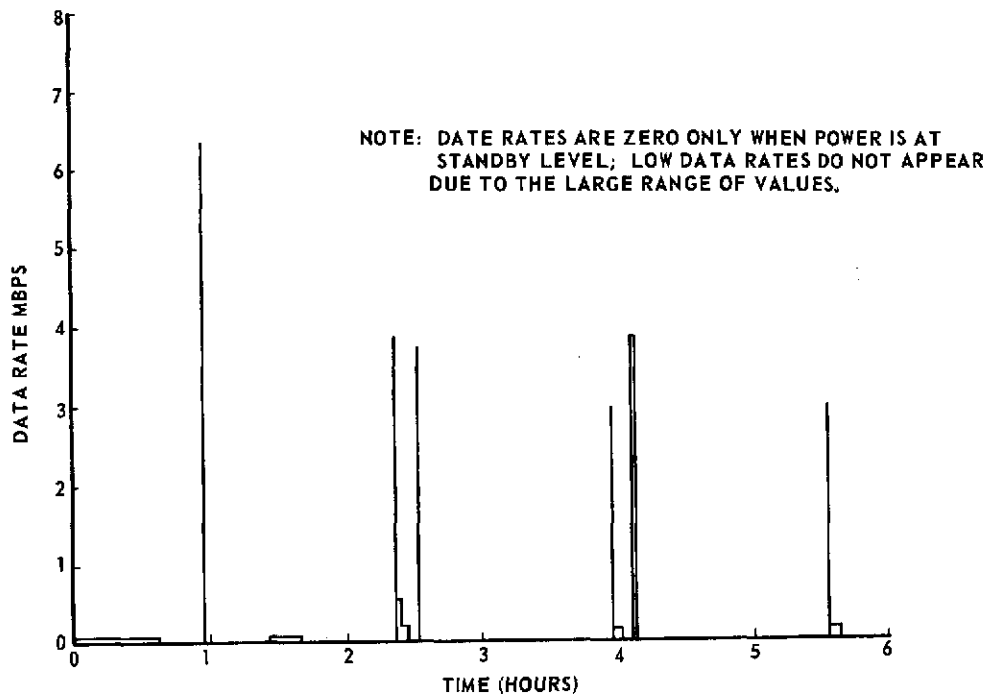
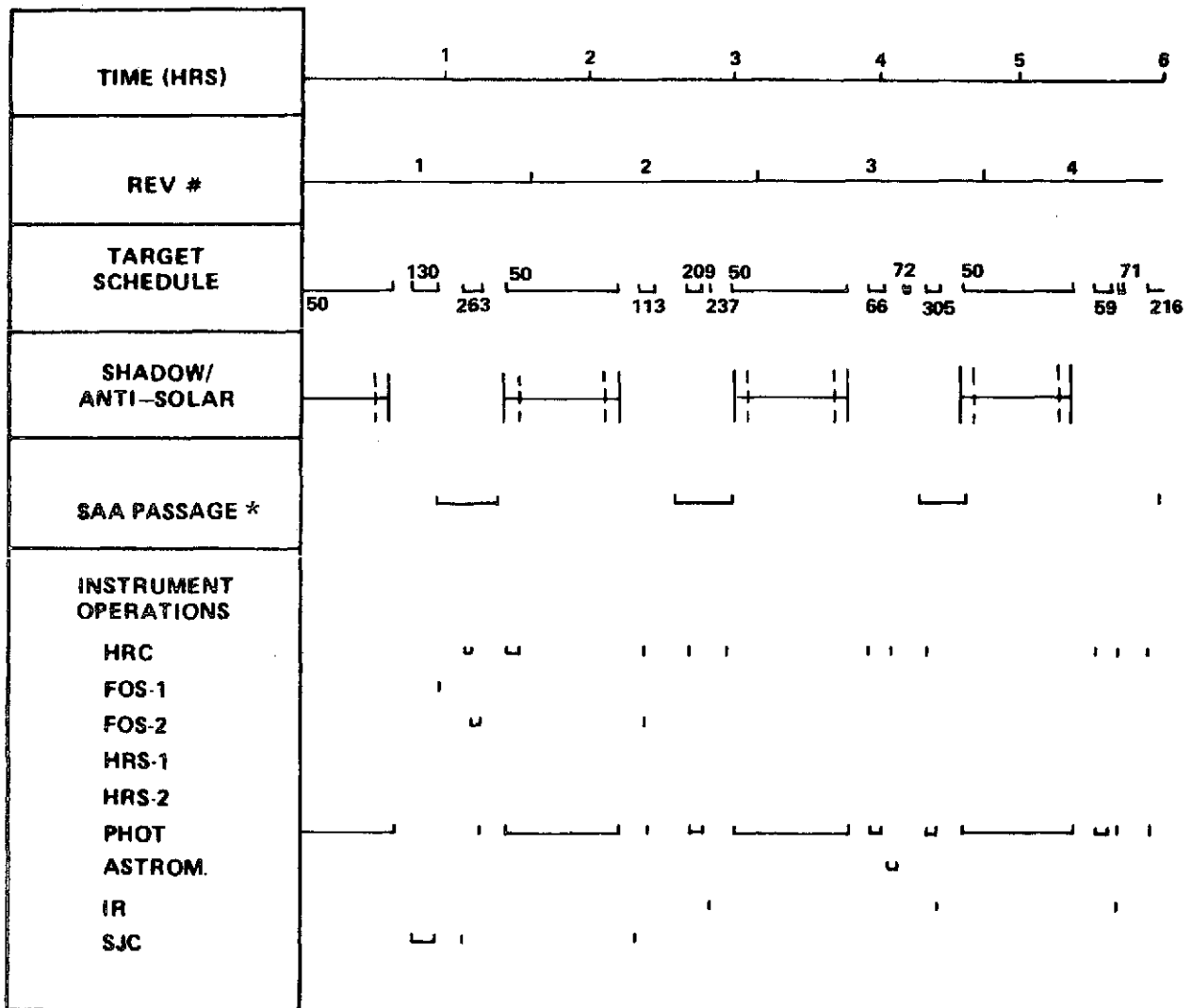


Figure 7. (Concluded).



*SOUTH ATLANTIC ANOMALY, 10 PROTONS/cm²/sec, ≥ 50 MeV

NOTE: EACH 6 HOUR MISSION SEGMENT IS PRESENTED IN A THREE PAGE FORMAT.

Figure 8. Option 2 timeline, TL-5.

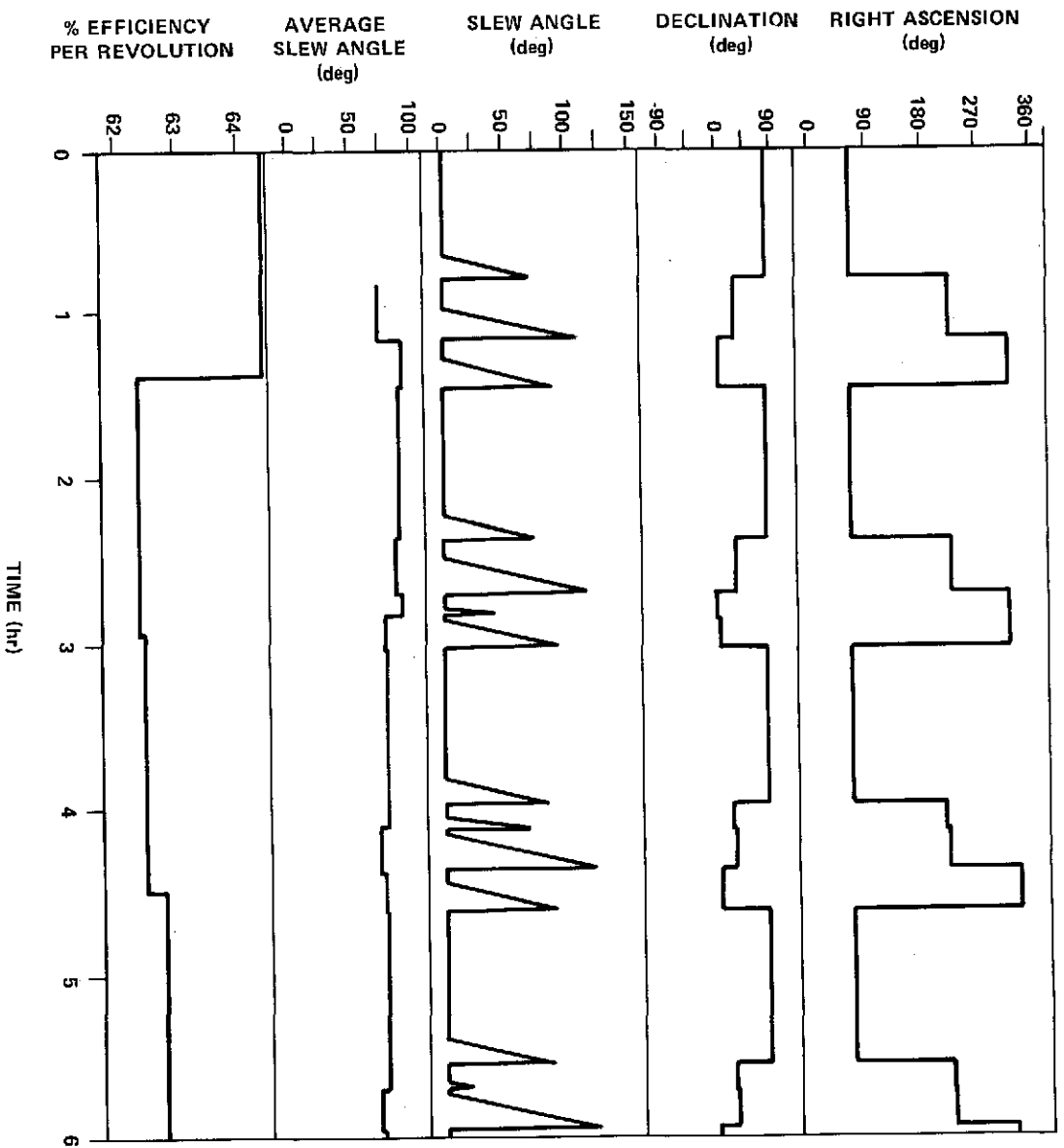


Figure 8. (Continued).

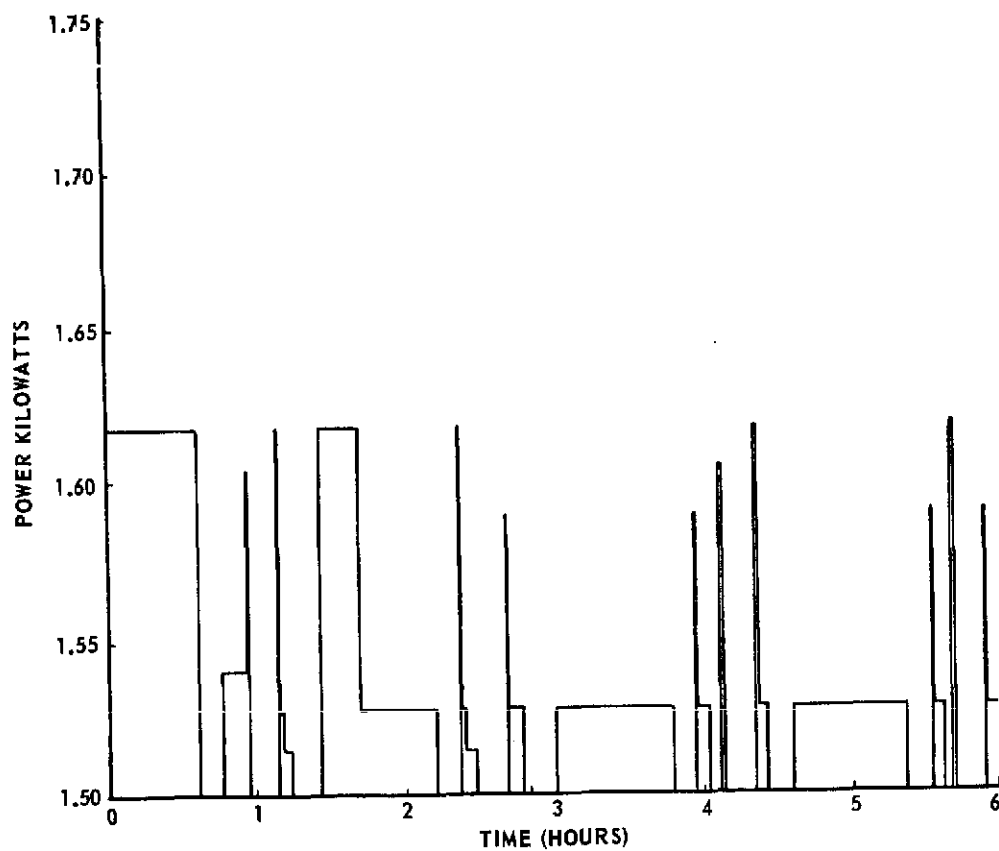
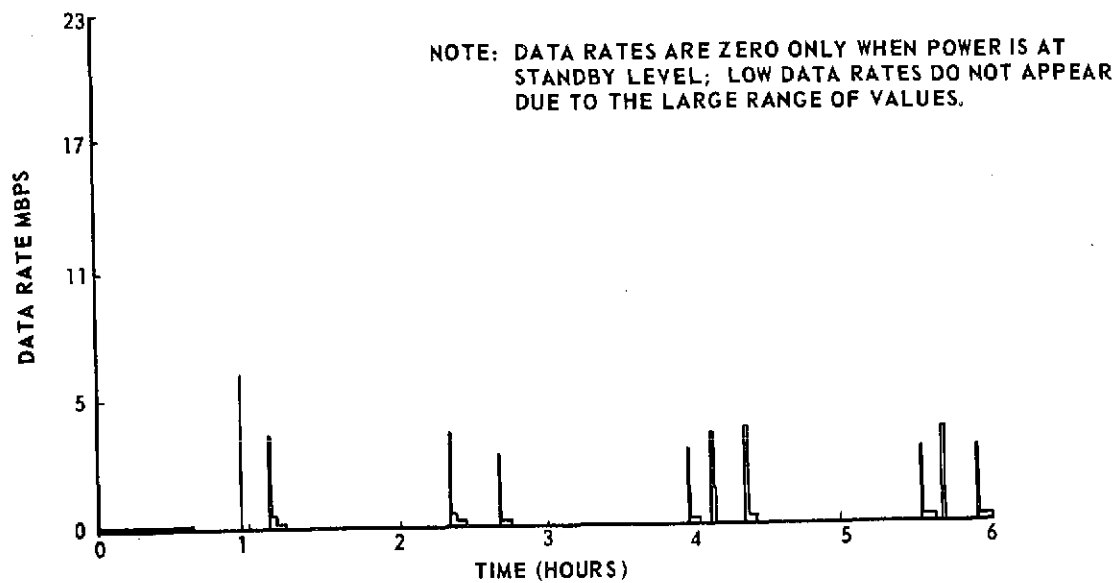


Figure 8. (Concluded).

E. Summary of Results and Statistical Analysis

A summary of quantitative results from the two DRM timelines is presented in Table 4. In addition to columns of statistics for options 1 and 2, a third column has been included to provide information relative to the prime viewing portion of the schedules to show how these statistics would change in the absence of secondary viewing. Recall that the prime viewing path is independent of the secondary path and is, therefore, the same in both options. Notice that although the slewing increases from 17 to 29 percent with the addition of region C, the total lost time actually decreases from 46 to 43 percent because of the large drop in waiting time. This waiting time is idle time when the telescope is not observing due to one of the following reasons: (1) there is not enough time left at the end of the secondary interval to view another target, (2) viewing another target causes a drop in optimum path value, or (3) no more target opportunities exist in the interval. In efficient schedules, waiting time can be driven to very low values and will occur only at the end of secondary viewing intervals, before a slew from one secondary region to another or from a secondary region back to the primary.

The foregoing statistics can be used to make a realistic estimate of the observation efficiency that can be achieved if baffling and other stray light protection devices provide target intervals that span the entire sun side of each revolution. This improvement in target availability will allow the elimination of region C, so the slew and settle times would be similar to those of option 1. For the same reason, waiting time would be no more than that of option 2, and probably less. This would give an overall efficiency of ~ 73 percent, or, in other words, a 23 percent increase in efficiency due to the addition of secondary viewing. The efficiency of any given revolution, of course, depends on the amount of slewing required and duration of secondary target observation. Since no relation exists between the scientific worth and viewing time required on a target, however, efficiency is not as important as the number of targets completed and viewing should, therefore, not be biased with respect to time.

Histograms of target magnitude, observation time, and slew time are presented in Figures 9 through 14.

TABLE 4. SUMMARY OF RESULTS FOR 2 DAYS (31 ORBITS)
OF OBSERVATIONS

Statistic	Option 1 (TL-4)	Option 2 (TL-5)	Prime Viewing Only
Number of Targets Completed	50	90	7
Average Number of Targets Completed per Revolution	1.61	2.90	0.23
Average Number of Targets Viewed per Revolution	2.58	3.90	1.16
Lost Time (%):			
Slew time	16.69	29.36	0.16
Settle time	5.42	8.19	0.35
Waiting time	23.89	5.08	49.58
Total	46.00	42.63	50.09
Observation Efficiency (%)	54.00	57.37	49.91
Efficiency Range per Revolution (%)	48.0 - 58.7	48.6 - 64.4	46.5 - 50.4
Number of Instrument Complements Scheduled	11	12	4
Number of Slews:			
Intra-region A	5	5	5
Intra-region B	13	9	—
Intra-region C	—	14	—
A-B (B-A)	30(30)	30	—
B-C	—	30	—
C-A	—	30	—
Total	78	118	5
Average Slew Angle (deg):			
Intra-region A	1.99	1.99	1.99
Intra-region B	7.71	5.26	—
Intra-region C	—	3.24	—
A-B (B-A)	84.4	84.0	—
B-C	—	129.2	—
C-A	—	100.4	—
Overall	66.56	81.44	1.99

TABLE 4. (Concluded)

Statistic	Option 1 (TL-4)	Option 2 (TL-5)	Prime Viewing Only
Average Slew Time (min):			
Intra-region A	0.9	0.9	0.9
Intra-region B	1.5	1.4	—
Intra-region C	—	1.1	—
A-B (B-A)	7.6	7.6	—
B-C	—	10.8	—
C-A	—	8.7	—
Overall	6.2	7.2	0.9
Maximum Slew Angle (deg)	94.1	155.7	2.4
Minimum Slew Angle (deg)	0.7	0.7	0.7
Total Path Length (deg)	5156.7	9611.1	10.0
Average Slew Distance per Revolution (deg)	166.3	310.04	0.32
Unused Prime Viewing Time (%)	0.51	0.51	0.51
Potential SAA Conflicts:			
Percentage of Time	1.63	2.82	1.35
Number of Targets Affected	10	22	2
Number of Data Frames Taken	103	183	15

IV. CONCLUSIONS

Timeline studies in support of the LST, Spacelab and Integrated Mission Planning Activity (IMAP) programs have demonstrated that the SCREAM algorithm is a valuable analysis tool. It has been applied in parametric studies to measure the performance of viewing philosophies and slew rate and to generate high fidelity mission simulations. The results of these simulations have been successfully used by subsystem designers to construct pointing and control momentum histories and assess thermal control, electrical power, and data management systems.

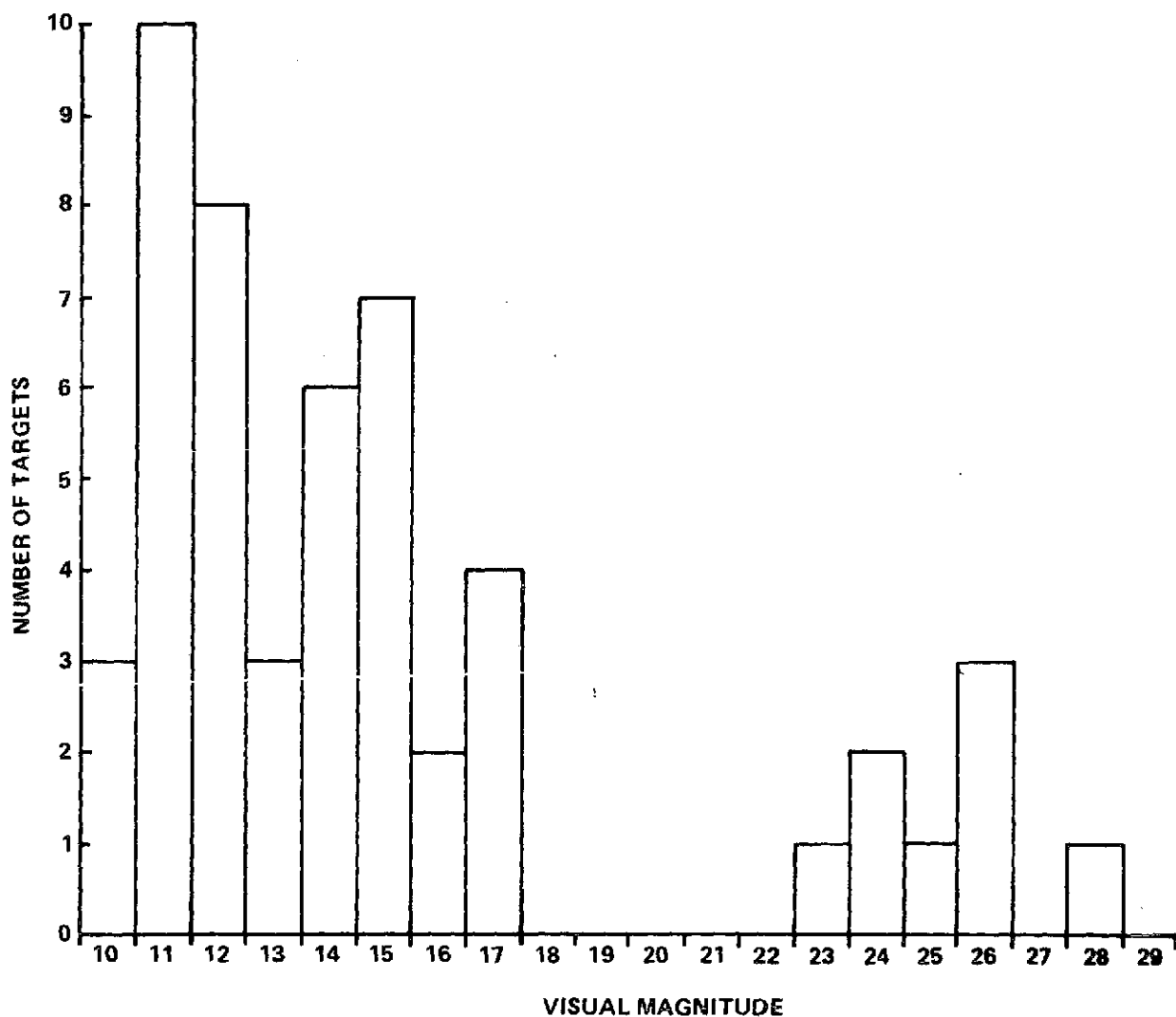


Figure 9. Distribution of targets scheduled in TL-4 according to magnitude.

Timeline algorithms such as SCREAM have numerous applications and can be effectively used in all phases of a project as a focal point for system requirements and constraints, to assess the impacts of guideline and subsystem performance changes and to eliminate the confusion that often surrounds decisions whose implications are too complex to determine without realistic simulations. This in turn, could save much valuable time and effort in spacecraft development.

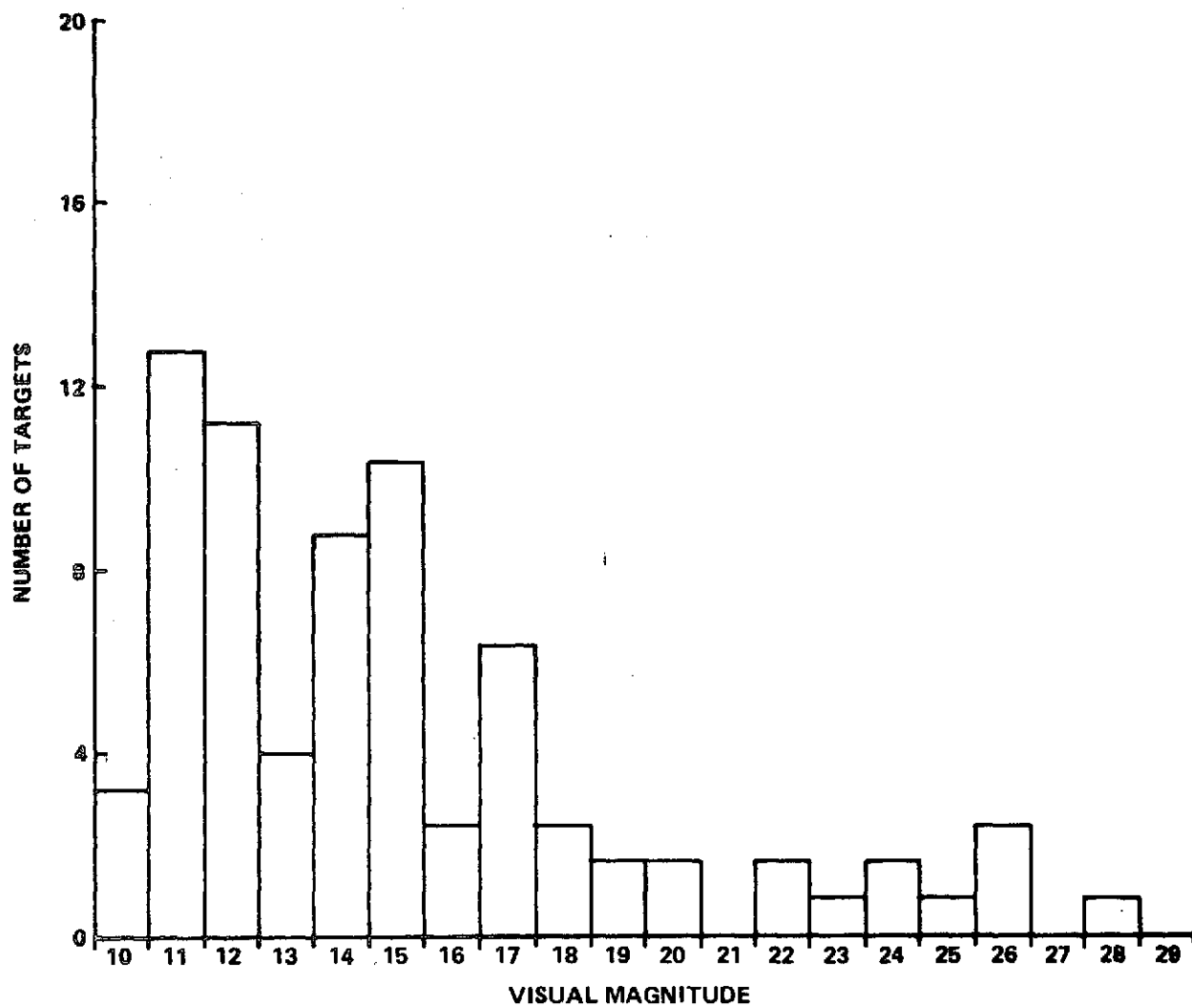


Figure 10. Distribution of targets scheduled in TL-5 according to magnitude.

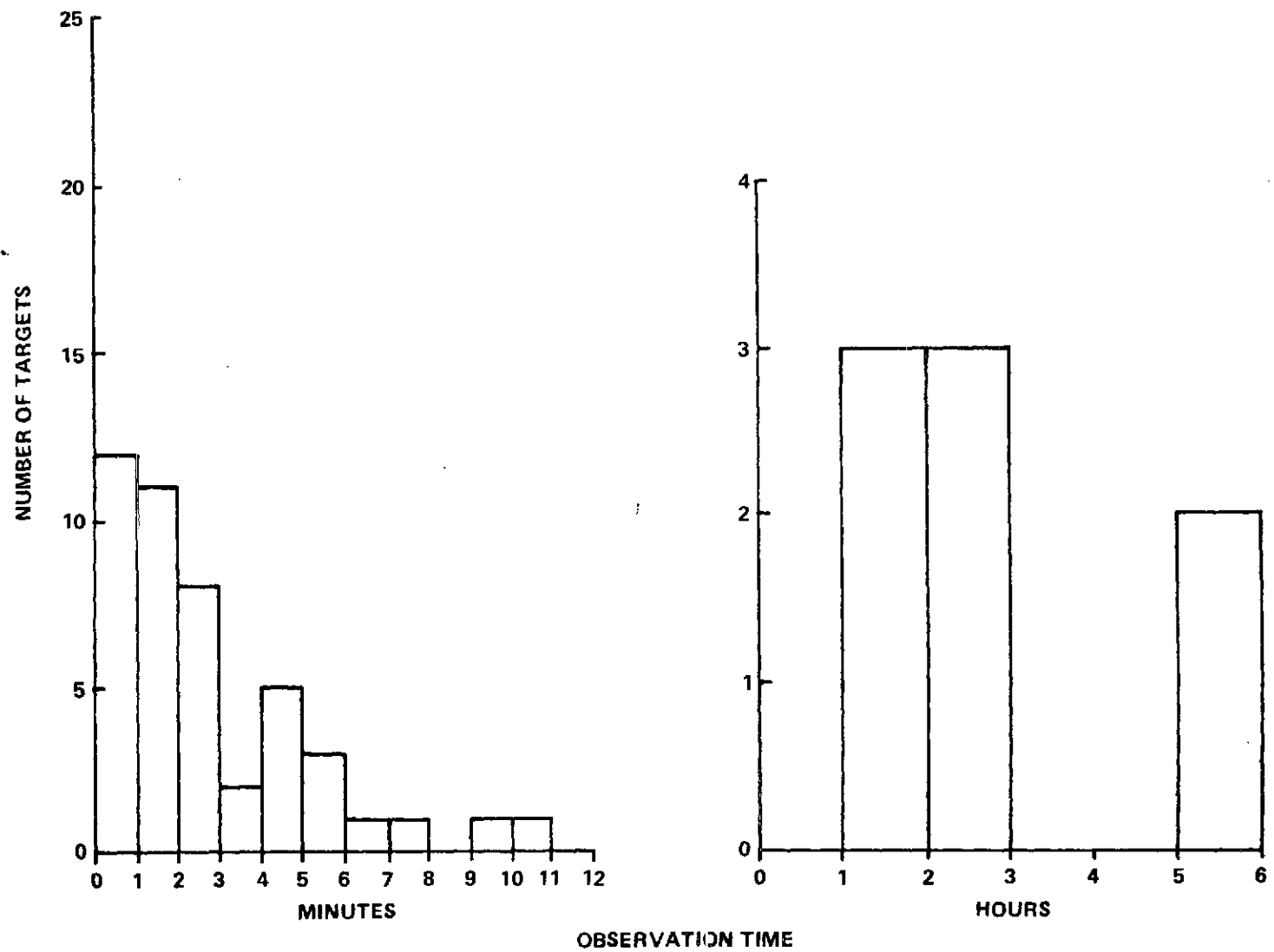


Figure 11. Distribution of observation times for TL-4.

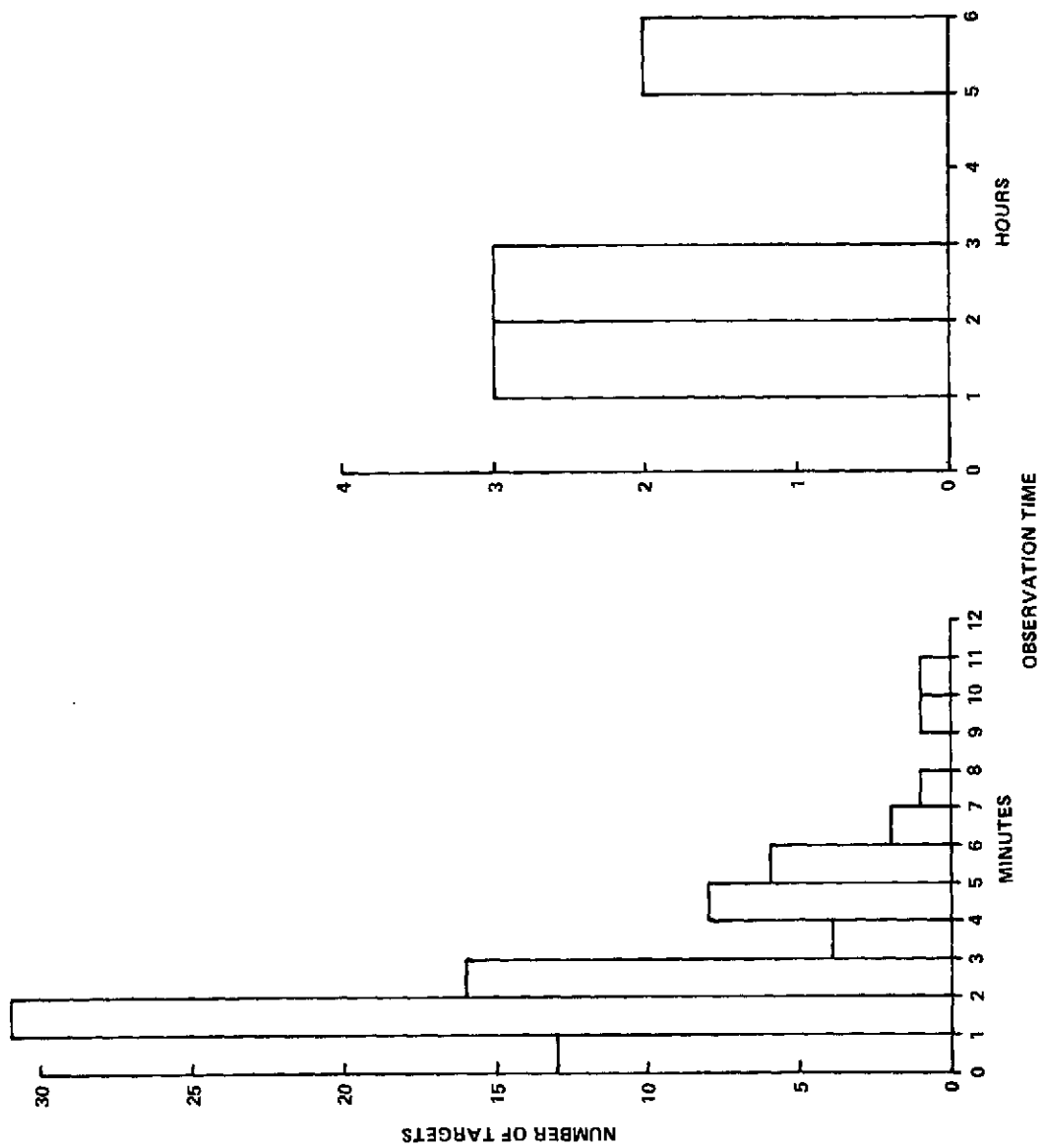


Figure 12. Distribution of observation times for TL-5.

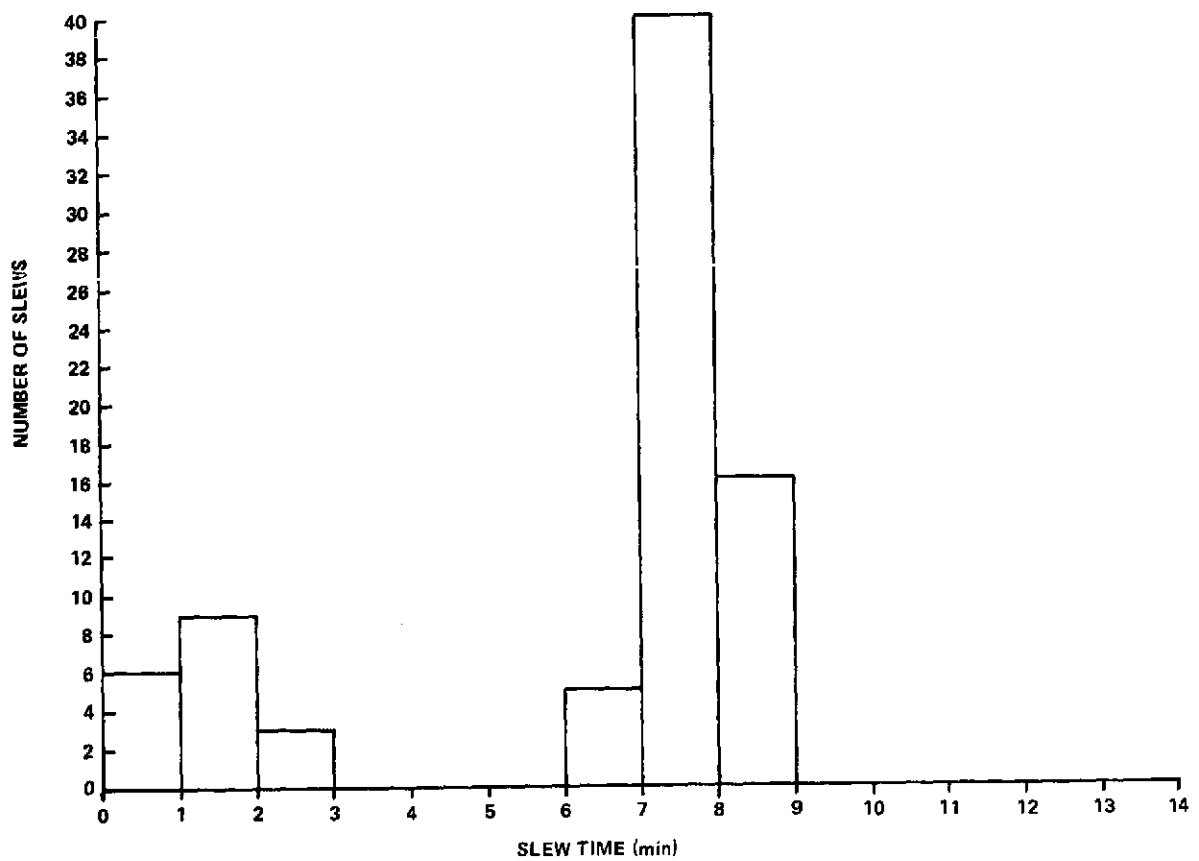


Figure 13. Distribution of slew times for TL-4.

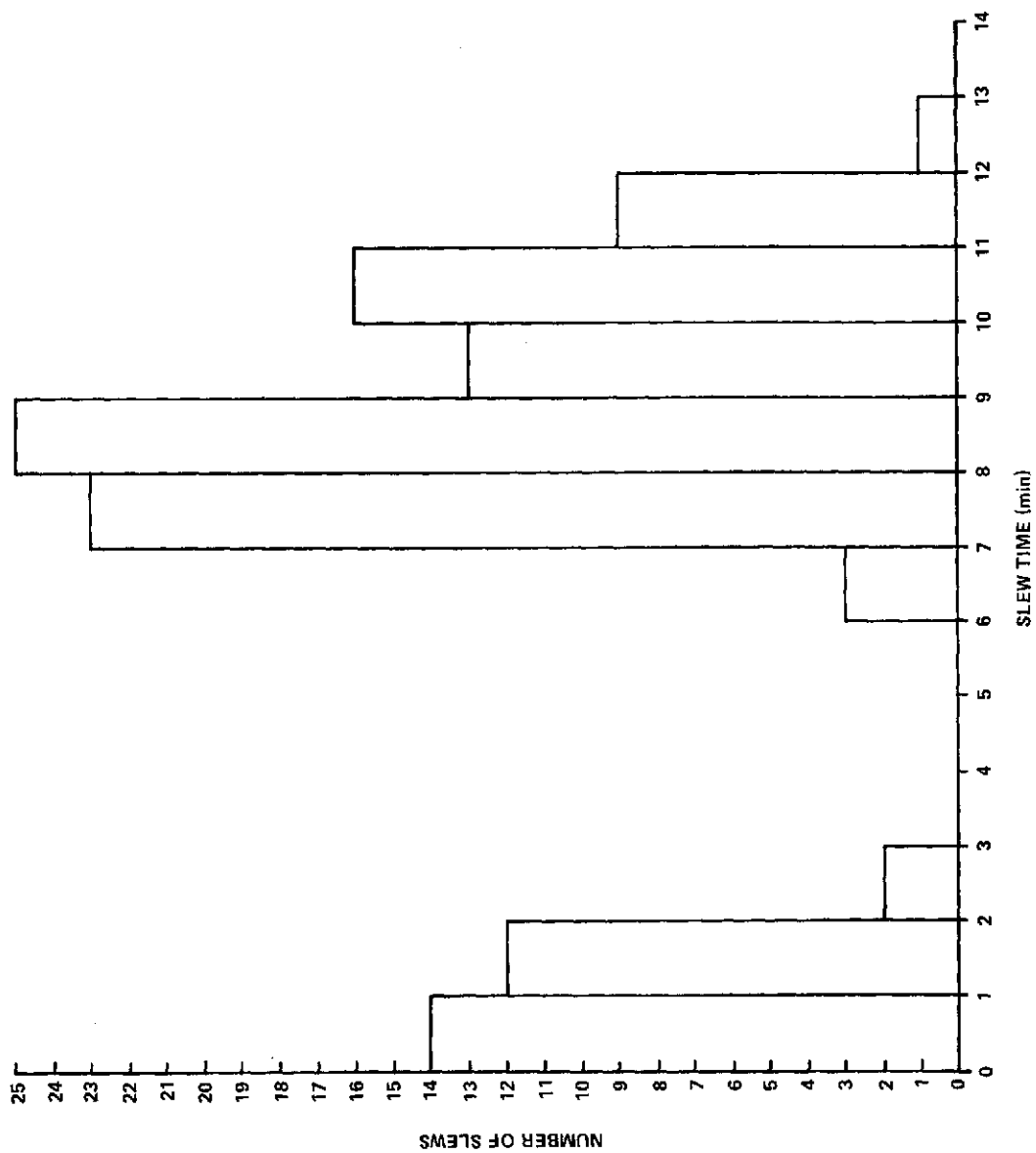


Figure 14. Distribution of slew times for TL-5.

APPENDIX

AN ALGORITHM FOR A SINGLE MACHINE SCHEDULING PROBLEM WITH SEQUENCE DEPENDENT SETUP TIMES AND SCHEDULING WINDOWS

The selection of stellar targets for a telescope in Earth orbit gave rise to the following scheduling problem.* One machine is available for performing tasks between times T_s and T_e . The machine can perform only one task at a time. There exist n candidate tasks numbered 1 through n from which a schedule for the period is to be developed. The performance of task i requires W_i time units and has a value of V_i for $i = 1, 2, \dots, n$. In addition, task i is constrained to be performed within the time period that begins at time B_i and ends at time E_i . The machine must be adjusted before the beginning of each task. The time required to adjust the machine following completion of task i before task j begins as A_{ij} . If task j is the first task in the sequence, then A_{0j} is the time required to adjust the machine. The problem is to select a feasible sequence of tasks to perform between times T_s and T_e which will maximize

$$Z = \sum_{i=1}^n X_i V_i$$

where $X_i = 1$ if task i is selected and $X_i = 0$ otherwise.

Let $S_{d_1}, S_{d_2}, \dots, S_{d_k}$ represent a general sequence containing k tasks where d_i represents the number of the i th task in the sequence. Define t_{d_i} to be the time when the performance of task d_i is to begin. The problem can now be stated formally as follows:

*Guffin, O. T. and Haussler, J. B.: Large Space Telescope Design Reference Mission Document. Marshall Space Flight Center, Sept. 1974 (Unpublished Report).

From the n candidate tasks, select a sequence of tasks $S_{d_1}, S_{d_2}, \dots, S_{d_k}$ which maximizes

$$Z = \sum_{i=1}^n V_{d_i}$$

subject to

1. $t_{d_i} \geq B_{d_i}$ for $i = 1, 2, \dots, k$.
2. $t_{d_i} + W_{d_i} \leq E_{d_i}$ for $i = 1, 2, \dots, k$.
3. $t_{d_1} \geq T_s + A_{0d_1}$.
4. $t_{d_i} + W_{d_i} + A_{d_i d_{i+1}} \leq t_{d_{i+1}}$ for $i = 1, 2, \dots, k-1$.
5. $t_{d_k} + W_{d_k} \leq T_e$.

This problem is very similar to the single machine job-shop problem with sequence dependent setup times [2] but it differs in two respects. First, the current problem is concerned with selecting an optimal subset of available tasks to schedule. In the job-shop problem, all available tasks are scheduled. The other distinction is that the performance of each task scheduled in the current problem is constrained to occur only within its particular time period. This constraint has no physical meaning in most job-shop problems.

Since a job-shop problem can be formulated as a linear integer programming problem [3-6], one would think that the current problem would have a similar formulation. However, consideration of the sequence dependent setup times and the selection of only a subset of the available tasks makes such a formulation very difficult. An enumeration algorithm similar to those used to solve zero-one integer problems was developed for solving the problem.

Solution Procedure

The algorithm implicitly enumerates only a portion of all feasible sequences while automatically discarding the remaining ones as nonpromising. The algorithm takes full advantage of the basic concepts employed by the Balas zero-one algorithm [7].

The algorithm contains two distinct parts:

1. A flexible enumeration scheme which records all sequences that have been considered and generates the remaining ones in a nonredundant fashion.
2. A number of tests for excluding from further consideration those sequences which either do not have a better objective value than the best sequence found so far, or are not feasible, or both.

Enumeration Scheme. An explanation of the enumeration scheme requires that the following definitions be introduced:

(i) Partial Sequence (J): This represents the first part of a sequence in which the first k tasks to be performed have been established. The notation $J = \{d_1, d_2, \dots, d_k\}$, $k < n$ is used to indicate that d_i is the i th task to be performed. A candidate task that is not contained in J is called a free task.

(ii) Completion of J: This is a complete sequence whose first k terms are defined by the partial sequence J . The notation $J_c = \{d_1, d_2, \dots, d_k, d_{k+1}, \dots, d_m\}$ denotes a completion of J . J_c is complete in the sense that no free task can be added to the end of the sequence without violating a constraint.

(iii) Fathomed Partial Sequence: A partial sequence is said to be fathomed if all of its completions can be discarded as nonpromising. Such completions may be either infeasible, or may not yield an improved value of the objective function, or both. Tests are applied to determine when a partial sequence is fathomed. These tests are called fathoming tests.

The enumeration scheme is based on the characteristic which distinguishes between two distinct sequences. Suppose $G = \{d_1, d_2, \dots, d_k\}$ and $H = \{h_1, h_2, \dots, h_m\}$ are two sequences. Then $G = H$ if and only if $m = k$ and $d_i = h_i$ for $i = 1, 2, \dots, k$. The enumeration scheme considers all possible sequences by generating a nonredundant sequence of partial sequences $J_0, J_1, J_2, \dots, J_k, J_{k+1}, \dots$ where J_{k+1} differs from each J_0, J_1, \dots, J_k in at least one position.

A number of variables will now be defined for use in explaining the procedure for generating a nonredundant sequence of partial sequences.

- r the number of positions in the current partial sequence J_k
- $J_k = \{d_1, d_2, \dots, d_r\}$ is the current partial sequence
- P_i number of free tasks which have been found to cause infeasibility when assigned to position i of J_k
- Q_j j th free task which cannot be assigned to a position for feasibility reasons; Q defines the specific tasks which are associated with P_i
- R_i number of candidate tasks that have been considered for i th position in J_k since the last time a task change occurred in any of positions $1, 2, \dots, i-1$
- H_{ij} i th candidate task which has been considered for j th position in J_k since a task change occurred in any of positions $1, 2, \dots, j-1$; variables R and H record which sequences have already been considered
- $N = \{1, 2, \dots, n\}$ is the set of all candidate tasks

The steps in the enumeration scheme can now be listed.

Step 1: Initiation

$J_k = \phi$, $r = 0$, $k = 0$ and $P_i = R_i = 0$ for $i \in N$.

Proceed to step 2.

Step 2: Apply fathoming test. Can J_k be fathomed? If no, continue to step 3. If yes and $r > 0$, go to step 5. Otherwise, go to step 8.

Step 3: Forward Move: Increment r by one. If $r = 1$, set $P_1 = 0$; otherwise set $P_r = P_{r-1}$. Define C to be the set of all free tasks excluding those defined by Q_i for $i = 1, 2, \dots, P_r$. If C is empty, go to step 6. Otherwise, for each

$\alpha \in C$, determine whether the sequence consisting of J_k with α augmented as its last element is feasible. For each α which causes the augmented sequence to be infeasible, increment P_r by one and set $Q_{P_r} = \alpha$. Is there an $\bar{\alpha} \in C$ which retains feasibility in augmented sequence? If yes, go to step 4. If no, go to step 6.

Step 4: $R_r = 1$ and $H_{1r} = \bar{\alpha}$. Form J_{k+1} by augmenting $\bar{\alpha}$ to J_k as its last element on the right. Add one to k and go back to step 2.

Step 5: Lateral Move: Define C to be the set of all free tasks excluding those defined by Q_i for $i = 1, 2, \dots, P_r$ and H_{jr} for $j = 1, 2, \dots, R_r$. If C is empty, go to step 6. Otherwise, for each $\alpha \in C$, determine whether the feasibility of J_k would be maintained if d_r is replaced by α . For each α that would cause infeasibility, increment P_r by one and set $Q_{P_r} = \alpha$. Is there an $\bar{\alpha} \in C$ which would maintain feasibility? If yes, go to step 7. If no, go to step 6.

Step 6: Backward Move: Decrement r by one. This deletes the right-most position of J_k . Is $r > 0$? If yes, go back to step 5 and attempt to select a replacement for d_r . If no, proceed to step 8.

Step 7: Form J_{k+1} by replacing d_r with $\bar{\alpha}$ from step 5. Increment R_r by one and set $j = R_r$. Set $H_{jr} = \bar{\alpha}$. This records the consideration of task $\bar{\alpha}$ for the r th position in current partial sequence. Increment k by one and return to step 2.

Step 8: Stop. All possible sequences have now been implicitly enumerated.

Note that the scheme is characterized by three basic steps: The forward move augments a free task on the right of the current partial solution; the lateral move replaces the task in the right-most position; and the backward move drops the right-most position. Schemes of this type are referred to as backtracking procedures.

The definitions of the variables P and Q may leave some doubt as to how they record infeasibility. Q_j for $j = 1, 2, \dots, P_i$ defines the tasks which cannot feasibly occupy position i . Q_j for $j = P_i + 1, P_i + 2, \dots, P_{i+1}$ defines the tasks which could feasibly occupy position i but would cause infeasibility in position $i + 1$. Notice that any task which would be infeasible in the i th position would also be infeasible in positions $i + 1, i + 2, \dots$. That is, if a task cannot be performed between times $t_{d_i} + W_{d_i}$ and T_e , then it certainly cannot be performed between times $T_{d_{i+m}} + W_{d_{i+m}}$ and T_e where m is a positive integer. This is the reason that $P_r = P_{r-1}$ at initiation of step 3.

The validity of the enumeration scheme is ascertained by the following theorem:

Theorem: (i) The completions of all future partial sequences do not duplicate any of the completions which have already been fathomed.

(ii) The scheme terminates only after all feasible sequences are considered.

Before providing a proof, a general description of the way in which the scheme operates will be given. In general, the scheme considers a group of feasible sequences at one time as opposed to considering one sequence at a time. A group of sequences is defined by a partial sequence in which the first r positions have already been assigned specific tasks. The completions of a partial sequence define the group of sequences to be considered. If the completions of a partial sequence are not fathomed, the number of completions under consideration is reduced by augmenting one more task to the partial sequence. The augmentation procedure is continued until the number of completions is small enough to be fathomed. At this point, the task in the last (r th) position of the partial sequence is replaced if a feasible and nonredundant replacement can be found. A replacement is nonredundant if it has not previously occupied this position since the task in the $(r - 1)$ position has been

replaced. The mechanics of the scheme insure that the tasks in positions $1, 2, \dots, r-2$ have not been replaced if the task in position $r-1$ has not been replaced. Thus replacing the task in the r th position insures that the next completions being considered are not redundant. If a feasible and nonredundant replacement for the r th position cannot be found, then all feasible completions of the current partial sequence with its last position deleted have been fathomed. The last position of current partial sequence is dropped and r is decremented by one. The task in the new r th position is replaced if a feasible and nonredundant replacement is available. If a replacement is available, the new set of completions being considered is nonredundant. Otherwise, the r th position is dropped and r decremented by one. The dropping of the last position is continued until either a position is reached for which a feasible and nonredundant replacement is available or r reaches the value of zero. When r becomes zero, all feasible completions have been implicitly enumerated.

Proof of Theorem: The proof will be by induction. The eight steps of the enumeration scheme will be referred to during the proof. The theorem is obviously true for $n = 1$. Assuming that it is true for $n = u$, we proceed to show that it is true for $n = u + 1$.

If the initial null partial sequence can be fathomed at step 2, the enumeration scheme is not used. So, we assume the process proceeds to step 3 after step 2. At step 3, a test is performed on each candidate task to determine if it can be feasibly performed as the first task in a sequence. Variables P and Q record which task cannot feasibly occupy the first position. If $P_1 > 0$, the problem reduces to one containing, at most, u tasks. This follows from the definition of the set C in steps 2 and 5. C can contain no more than $u + 1 - P_r$ tasks where $P_r \geq P_1$ for $r > 0$. Thus, if the method can fail, it can only do so when $P_1 = 0$ at the end of step 3. In this case any one of the $u + 1$ tasks could feasibly occupy the first position. One is selected and assigned to the first position to form J_1 at step 4. The assignment of this particular task to the first position is recorded by variables R and H . The problem is now temporarily reduced to one containing u tasks since the task just assigned is removed from the list of free tasks.

By the induction hypothesis, the enumeration scheme considers all feasible sequences of the u task problem without duplication. Termination of this problem occurs at step 6 when r is reduced once again to a value of 1. The process now proceeds to step 5 to locate a replacement for the task initially assigned to the first position.

At step 5, the candidate tasks from which the replacement is to be chosen are defined by the set C . Since we established at step 3 that $P_1 = 0$, C contains all $u + 1$ tasks except the one recorded by the R and H variables. (Note that P_1 will retain a value of zero because we assumed above that each of the $u + 1$ tasks could feasibly occupy the first position in a sequence.) This means that the task chosen for the first sequence position will be different for the one initially assigned to this position. Therefore, all completions of J_1 which have already been fathomed will not be duplicated by any completions of the new partial sequence that is created at step 7.

The assignment of another task to the first position has once again temporarily reduced the problem to one involving u tasks. The process now returns to step 2 and begins consideration of this u task problem. By hypothesis, the process considers all feasible sequences of this u task problem without duplication. Termination occurs at step 6 when r is reduced to a value of 1. Once again a replacement for the task in the first position is selected at step 5. Since the first two variables considered for the first position were recorded by the R and H variables at steps 4 and 7, the task chosen at step 5 will be one not previously considered for the first position. Therefore, the completions of the new partial sequence will not duplicate any of those that have already been fathomed. The problem has again reduced to one containing u tasks at step 7.

The scheme has now begun to follow a set iterative pattern. The termination of a u task problem occurs at step 6 when r is decremented to a value of 1. A replacement for the task assigned to the first position is chosen at step 5. At step 7, the chosen task is assigned the first position and its assignment is recorded by R and H variables. This establishes a new u task problem.

To establish that the scheme considers all feasible sequences in a non-redundant way before terminating, notice that at step 5 the replacement task is always chosen from among those tasks not previously assigned to the first position. This is assured by the use of the R and H variables in establishing the set C . Since $P_1 = 0$, C always contains all tasks not previously assigned to the first position. This means that C will be empty and cause the scheme to terminate only after all $u + 1$ tasks have been previously assigned to the first position. This completes the proof, since the first sequence position can only be assigned in the $u + 1$ distinct ways that have been considered in this process, and, by assumption, in each of the $u + 1$ cases that the method handles the resulting u task problem as specified by the theorem.

Fathoming Tests. The fathoming tests determine whether J_k has any promising completions. If none exist, the lateral move of the enumeration scheme occurs, and additional fathoming tests determine which task should be considered next for the r th position in J_k . If all completions of J_k cannot be shown to be nonpromising, other fathoming tests determine which task should be augmented to J_k during the forward move.

Before proceeding to describe the fathoming test applied at step 2, three additional variables need to be defined. Let Z_b be the value of the best sequence at present. Define Z_k to be the value of J_k , that is, $Z_k = \sum_{i=1}^r V_{d_i}$. Define T_r to be time when performance of task d_r is completed. These three variables will now be used to explain the fathoming mechanism.

As stated above, the fathoming test determines whether J_k has any promising completions. The determination is made by computing the highest possible value, \bar{Z}_k , any completion of J_k could attain. If $\bar{Z}_k \leq Z_b$, then J_k will be fathomed. Otherwise, J_k is not fathomed.

\bar{Z}_k is computed by first determining which free tasks would be feasible candidates for occupying positions $r+1, r+2, \dots$ in any completion of J_k . Since any task that could feasibly occupy position $r+1$ could possibly occupy positions $r+2, r+3, \dots$, the list of candidates is restricted to those which could occupy position $r+1$. Next, these candidates are ordered according to their ratio of completion value, V_i , to performance time, W_i . The candidate having the largest ratio is placed in first position of order. For simplicity of notation, let $1, 2, 3, \dots, m$ be the ordered list of candidate tasks. Next, compute $M = \min \{A_{d_r i} | i = 1, 2, \dots, m\}$. M is the minimum setup time between task d_r and any one candidate task. Consider the sequence which places task 1 in position $r+1$ of J_k with a setup time of M , task 2 in position $r+2$, etc., until all of the time between T_r and T_e has been filled. Define $U = T_e - T_r$. Then tasks $1, 2, \dots$, are placed respectively in positions $r+1, r+2, \dots$ until $X = U - M - W_1 - W_2 - \dots - W_q \geq 0$ and

$X - W_{q+1} < 0$. Task $q + 1$ is placed in position $r + q + 1$ and a value of $X(V_{q+1}/W_{q+1})$ is assumed for its performance value. The value of the best possible completion of J_k could not exceed the value of this sequence.

\bar{Z}_k is computed as follows:

$$\bar{Z}_k = Z_k + \sum_{i=1}^q V_i + (X/W_{q+1}) V_{q+1} .$$

For example, suppose $M = 1$, $U = 17$, $W_1 = 7$, $W_2 = 7$, $W_3 = 5$, $W_4 = 6$, $V_1 = 24$, $V_2 = 14$, $V_3 = 8$, and $V_4 = 6$. Then tasks 1, 2 and 3 are placed in positions $r + 1$, $r + 2$, and $r + 3$, respectively. Since there is only time to perform task 3 for two time units, its performance value is reduced to $(2/5) 8 = 3.2$. Then

$$\bar{Z}_k = Z_k + 24 + 14 + 3.2 .$$

The execution of either the forward move (step 3) or the lateral move (step 5) requires that a task be chosen for augmentation or replacement, respectively. In either case, a heuristic rule for selecting the most "promising" task is used. Intuitively, this task should provide a maximum amount of value and require a minimum amount of setup, waiting, and performance time. This is equivalent to choosing the task with the maximum ratio of value (V_i) to total (setup plus waiting plus performance) time. If the period of time between T_{r-1} and the time the i th candidate task can begin (B_i) is longer than the setup time ($A_{r-1 i}$), the machine would be idle for $B_i - A_{r-1 i} - T_{r-1}$ time units. The waiting time associated with the i th candidate task is therefore $\max(0, B_i - A_{r-1 i} - T_{r-1})$. The ratio for the i th candidate task is

$$\frac{V_i}{W_i + A_{r-1 i} + \max(0, B_i - A_{r-1 i} - T_{r-1})} .$$

An Example. The operation of a machine is to be scheduled between times $T_s = 0$ and $T_e = 20$. There exist three candidate tasks from which a schedule is to be developed. The following matrix lists the characteristics of each task:

Task	W_i	V_i	B_i	E_i	A_{0j}
1	8	12	11	22	3
2	5	3	3	11	4
3	7	5	4	17	2

The following matrix defines the sequence dependent setup time (A_{ij}):

		Task j →		
Task i ↓		1	2	3
	1	0	4	2
	2	3	0	1
	3	1	2	0

The eight steps of the enumeration schemes will be referred to as the algorithm is applied.

Step 1: Initiate variables.
Set $r = 0$, $k = 0$, $J = \phi$,
 $Z_0 = 0$, $Z_b = -\infty$, $Z_k = 0$
and $T_r = T_s = 0$. Proceed
to step 2.

Step 2: Apply fathoming test. Since $Z_0 > Z_b$, J_0 cannot be fathomed. Continue to step 3.

Step 3: Select a task to augment to J_0 . Set $r = 1$, $P_1 = 0$ and $C = \{1, 2, 3\}$. For each $y \in C$, determine whether the sequence consisting of J_0 with y as its only task is feasible. The sequence consisting of task 1 is feasible since $A_{01} + T_0 < B_1$ and $B_1 + W_1 < T_e < E_1$. Also, the sequence consisting of task 2 is feasible since $T_0 + A_{02} > B_2$ and $T_0 + A_{02} + W_2 < E_2 < T_e$. Similarly, the sequence consisting of task 3 is feasible.

The value to total time ratio

$$\frac{V_i}{W_i + A_{r-1 i} + \max(0, B_i - A_{r-1 i} - T_{r-1})}$$

is now computed for each $y \in C$ to determine which of the three tasks to augment to J_0 . The ratios for tasks 1, 2, and 3 are

$$\frac{12}{8+3+8}, \quad \frac{3}{5+4+0}, \quad \text{and} \quad \frac{5}{7+2+2}, \quad \text{respectively.}$$

Task 1 is selected since it has the largest ratio. Proceed to step 4.

- Step 4: Augment task 1 to J_0 . Set $k = 1$, $R_1 = 1$, $H_{11} = 1$, $J_1 = \{1\}$, $Z_1 = 12$, $t_1 = 11$, and $T_1 = 19$. Go to step 2.
- Step 2: Apply fathoming test. First determine the free tasks that could be feasibly augmented to J_1 . Tasks 2 and 3 are the free tasks, but neither of them could be feasibly augmented to J_1 because $T_1 > E_2$ and $T_1 > E_3$. Therefore, J_1 is a complete sequence. Set $Z_b = Z_1 = 12$. J_1 is fathomed since it has no more promising completions. Proceed to step 5.
- Step 5: Select a replacement for task 1 in J_1 . Since $P_1 = 0$, $R_1 = 1$ and $H_{11} = 1$, $C = \{2, 3\}$. Tasks 2 and 3 are both feasible replacements. The value to total time ratios for tasks 2 and 3 are $3/9$ and $5/11$, respectively. Therefore, task 3 is chosen to replace task 1. Proceed to step 7.
- Step 7: Set $k = 2$, $J_2 = \{3\}$, $R_1 = 2$, $H_{21} = 3$, $t_3 = 4$, $T_1 = 11$, and $Z_2 = 5$. Go to step 2.
- Step 2: Apply fathoming test. First determine the free tasks that could be feasibly augmented to J_2 . Tasks 1 and 2 are the free tasks. Task 1 can be feasibly augmented since $T_1 + A_{31} > B_1$ and $T_1 + A_{31} + W_1 = T_e < E_1$. Task 2 cannot be feasibly augmented since $T_1 + A_{32} > E_2$. Compute $\bar{Z}_2 = Z_2 + V_1 = 17$. J_2 is not fathomed since $\bar{Z}_2 > Z_b$. Continue to step 3.
- Step 3: Set $r = 2$, $P_2 = P_1 = 0$, and $C = \{1, 2\}$. In the previous step, we learned that task 1 could be feasibly augmented to J_2 , but task 2 could not be feasibly augmented. Set $P_2 = 1$ and $Q_1 = 2$. Proceed to step 4.

- Step 4: Set $k = 3$, $J_3 = \{3, 1\}$, $R_2 = 1$, $H_{12} = 1$, $Z_3 = 17$, $t_1 = 12$, and $T_2 = 20$. Go to step 2.
- Step 2: Task 2 is the only free task and it cannot be feasibly augmented to J_3 since $T_2 > E_2$. This means that J_3 is a complete sequence, so it is fathomed. Set $Z_b = Z_3 = 17$ and go to step 5.
- Step 5: Since $P_2 = 1$, $Q_1 = 2$, $R_2 = 1$, and $H_{12} = 1$, C is null. Continue to step 6.
- Step 6: Set $r = 1$, $J_3 = \{3\}$, $t_3 = 4$, $T_1 = 11$, and to to step 5.
- Step 5: Attempt to find a replacement for task 3 in J_3 . Since $R_1 = 2$, $H_{11} = 1$, $H_{21} = 3$, and $P_1 = 0$, $C = \{2\}$. Task 2 can feasibly replace task 3. Since it is the only task in C , it is selected to replace task 3. Proceed to step 7.
- Setp 7: Set $k = 4$, $J_4 = \{2\}$, $R_1 = 3$, $H_{31} = 2$, $t_2 = 4$, $T_1 = 9$, and $Z_4 = 3$. Go to step 2.
- Step 2: Apply fathoming test. First determine the free tasks that could be feasibly augmented to J_4 . Tasks 1 and 3 both satisfy this condition. Next, order these two tasks according their V_i/W_i ratios. Task 1 is placed in first position since it has the largest ratio. The minimum setup time between task 2 and either task 1 or task 3 is 1, so $M = 1$. Compute $U = T_e - T_1 = 11$. Since $X = U - M - W_1 > 0$ and $X - W_3 < 0$,
- $$\bar{Z}_4 = Z_4 + V_1 + X(V_3)/W_3 = 16 + 3/7 \quad .$$
- J_4 is fathomed because $\bar{Z}_4 < Z_b = 17$. Go to step 5.
- Step 5: Attempt to find a replacement for task 2 in J_4 . C is null because $R_1 = 3$, $H_{11} = 1$, $H_{21} = 3$, and $H_{31} = 2$. Continue to step 6.
- Step 6: Set $r = 0$. Proceed to step 8.
- Step 8: Stop. All possible sequences have now been implicitly enumerated.

The optimum sequence is given by $J_3 = \{3, 1\}$ with $Z_b = 17$. Notice that it was identified without enumerating all feasible sequences.

Computational Experience

The algorithm is currently being used to support the design of a telescope to be operated in Earth orbit. Typical observational timelines are developed and used in the design of the telescope's pointing, maneuvering, data management, and other subsystems.

An observational timeline specifies the time sequence in which targets are to be viewed over several orbits of the telescope. The telescope is shaded from sunlight by the Earth for a portion of each orbit. This period is always used to observe a very faint target. Each faint target scheduled must be viewed during the shadow portion of several consecutive orbits to complete data collection. Brighter targets are viewed during the remainder of each orbit. Since the brighter targets require only a short time span to complete data collection, several of them may be viewed during the sunlight portion of an orbit. The problem of selecting a sequence of bright targets to view during the sunlight portion of one orbit coincides with the sequencing problem presented in this paper. The scheduling routine used to generate a timeline for several orbits employs the algorithm presented herein to develop a timeline for the sunlight portion of each orbit.

The algorithm was implemented in a Fortran IV code for a Univac 1108 computer. To obtain computational experience, the code was used to generate a timeline for the sunlight portion of 10 typical orbits of the telescope. Each of the 10 timelines was generated from a different list of 200 bright targets. The number of targets per optimum timeline ranged between 6 and 10. The computational time, excluding input and output times, per timeline ranged from 0.61 sec to 0.80 sec with a mean of 0.71 sec. The same 10 problems were rerun after the size of each candidate list of bright targets had been reduced to 150. The computational times ranged from 0.38 to 0.42 sec with a mean of 0.40 sec. Just as one would expect, the size of the target list has a significant influence on computational time. Additional computational experience indicates that computational time also increases as the number of targets in the optimal sequence increases.

Other Potential Applications

The algorithm is presently being considered for use in scheduling the daily activities of a crewman during a space mission. There usually exist many more daily tasks, not all of which are mandatory, than a crewman can perform. The value or priority of the different tasks vary. In addition, the performances of many tasks are constrained to occur within particular time windows due to target availability, housekeeping requirements, etc. (If task i does not have a scheduling window, set $B_i = T_s$ and $E_i = T_e$.) Frequently, as

during the Skylab mission, a crewman will have to refer to a manual (set himself up) before performing the task. These constraints are considered by the algorithm. However, this problem usually has additional constraints such as equipment conflicts, consumable constraints, and crewman availability. An extension of the algorithm is presently being developed to consider these constraints. Similarly, one person scheduling problems, such as the sharing of a quality inspector among several departments, may exist outside of NASA.

REFERENCES

1. Gary, G. A. and Craven, P. D.: A Study of Zodiacal Light Models. NASA TN D-7263, June 1973.
2. Conway, R. W.; Maxwell, W. L.; and Miller, L. W.: Theory of Scheduling. Addison-Wesley, 1967.
3. Bowman, E. H.: The Schedule-Sequencing Problem. Operations Research, vol. 7, no. 5, Sept. - Oct. 1959.
4. Wagner, H.: An Integer Linear Programming Model for Machine Scheduling. Naval Research Logistics Quarterly, vol. 6, no. 2, June 1959.
5. Manne, A. S.: On the Job-Shop Scheduling Problem. Operations Research, vol. 8, no. 2, Mar. - Apr. 1960.
6. Pritsker, A. A. B.; Watters, L. J.; and Wolfe, P. M.: Multiproject Scheduling with Limited Resources: A Zero-One Programming Approach. Management Science, vol. 16, no. 1, Sept. 1969.
7. Glover, F.: A Multiphase-Dual Algorithm for the Zero-One Integer Programming Problem. Operations Research, vol. 13, no. 6, Nov. - Dec. 1965.

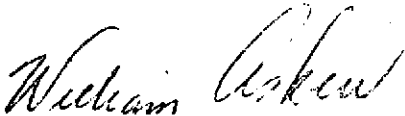
APPROVAL

A TIMELINE ALGORITHM FOR ASTRONOMY MISSIONS

By John E. Moore and Orville T. Guffin

The information in this report has been reviewed for security classification. Review of any information concerning Department of Defense or Atomic Energy Commission programs has been made by the MSFC Security Classification Officer. This report, in its entirety, has been determined to be unclassified.

This document has also been reviewed and approved for technical accuracy.



WILLIAM C. ASKEW

Chief, Mission Integration Branch



JAMES P. LINDBERG

Chief, Mission Analysis Division



HERMAN E. THOMASON

Director, Systems Analysis and Integration Laboratory